# Recent Results from HERA ep Collisions

François Corriveau, IPP/McGill

on behalf of the H1 and ZEUS Collaborations

Pascos07 at ICL, London

3 July 2007

- H1 and ZEUS at HERA
- Proton structure functions
- Polarisation at HERA
- A few of the Searches
- QCD Studies
- Outlook

Athena ZEUS Hera

HERA

# HERA Physics Topics

**Electroweak**

**Structure Functions**

**QCD**

*Heavy Flavour*

*Hadronic Final States*

..

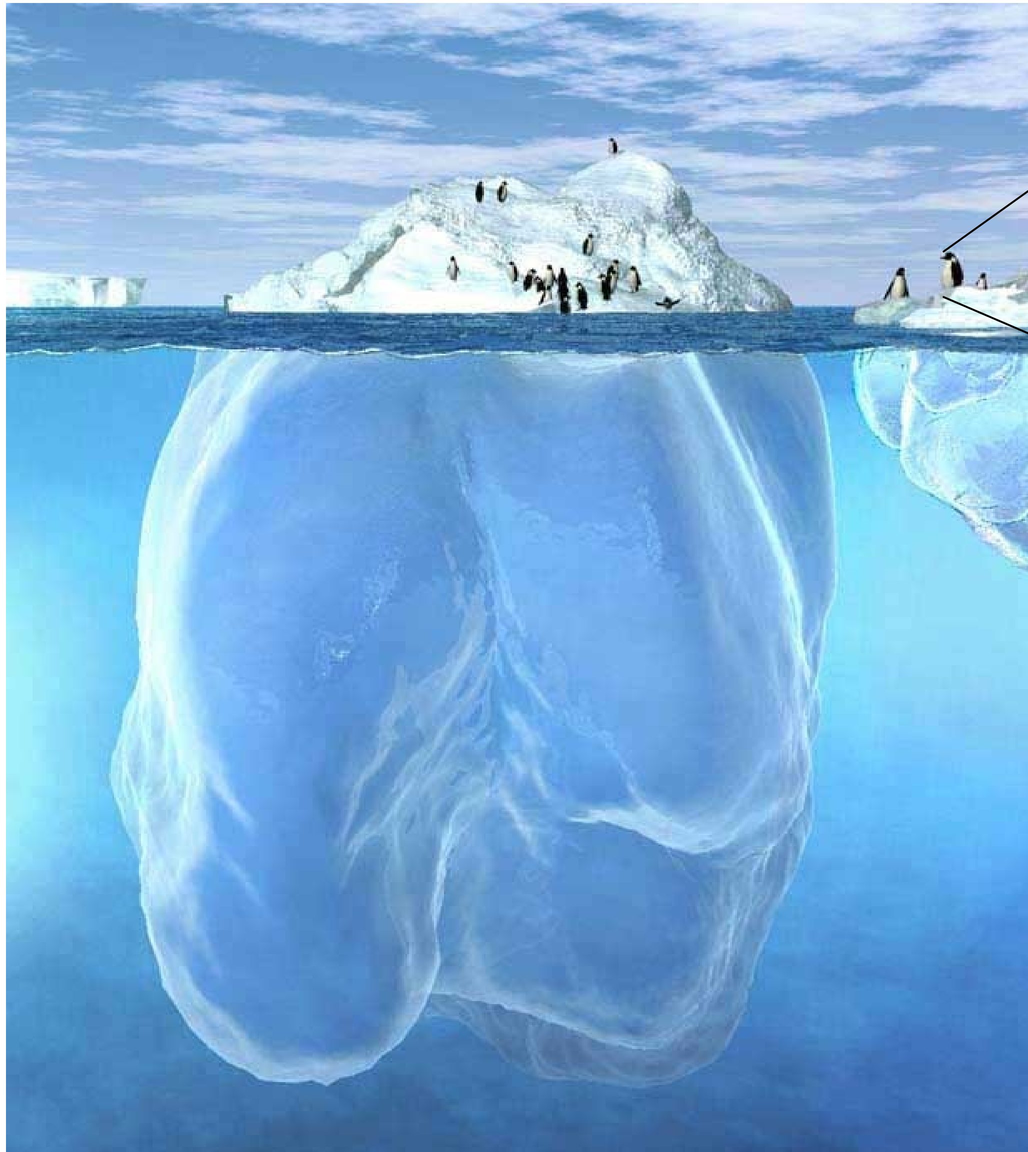

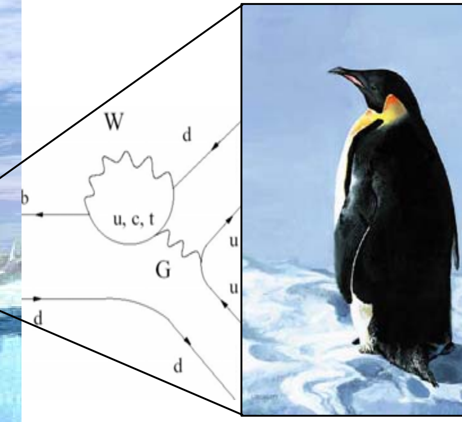


**Searches**, *Exotics, Rare Phenomena, ..*

*Vector Mesons*

*Diffraction*

..

# ep - Kinematics

27.6 GeV electrons/positrons on 920 GeV protons

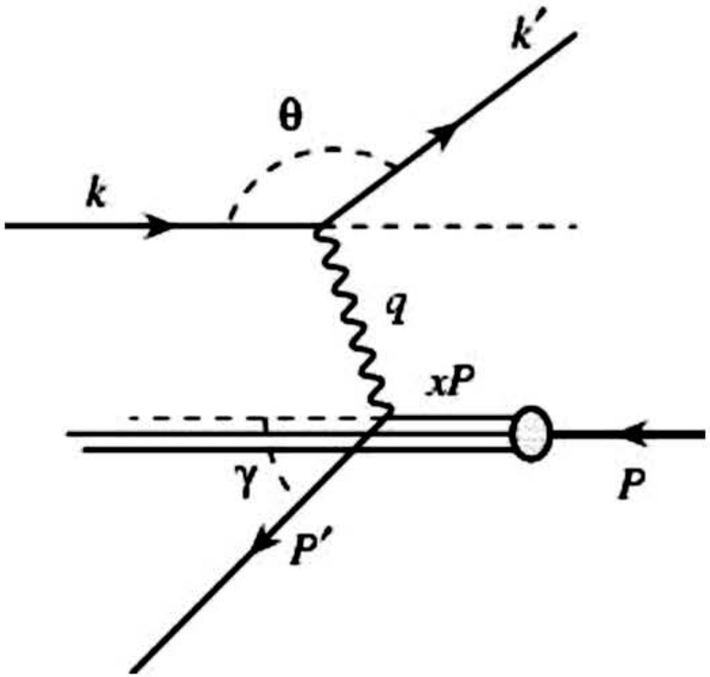


$$Q^2 = -q^2 = -(k-k')^2$$

$$x = \frac{Q^2}{2p \cdot q} \qquad y = \frac{p \cdot q}{p \cdot k}$$

$$s = (p+k)^2 \qquad Q^2 = x \cdot y \cdot s$$

$Q^2$ = exchanged momentum (squared)

x = Bjorken scaling variable

y = inelasticity scaling variable

$\sqrt{s}$ = center of mass energy (~320 GeV)

**Deep Inelastic Scattering (DIS):**

Neutral current (NC) via $\gamma/Z^0$ exchange

Charged current (CC) via $W^\pm$ exchange

# DIS NC & CC Events

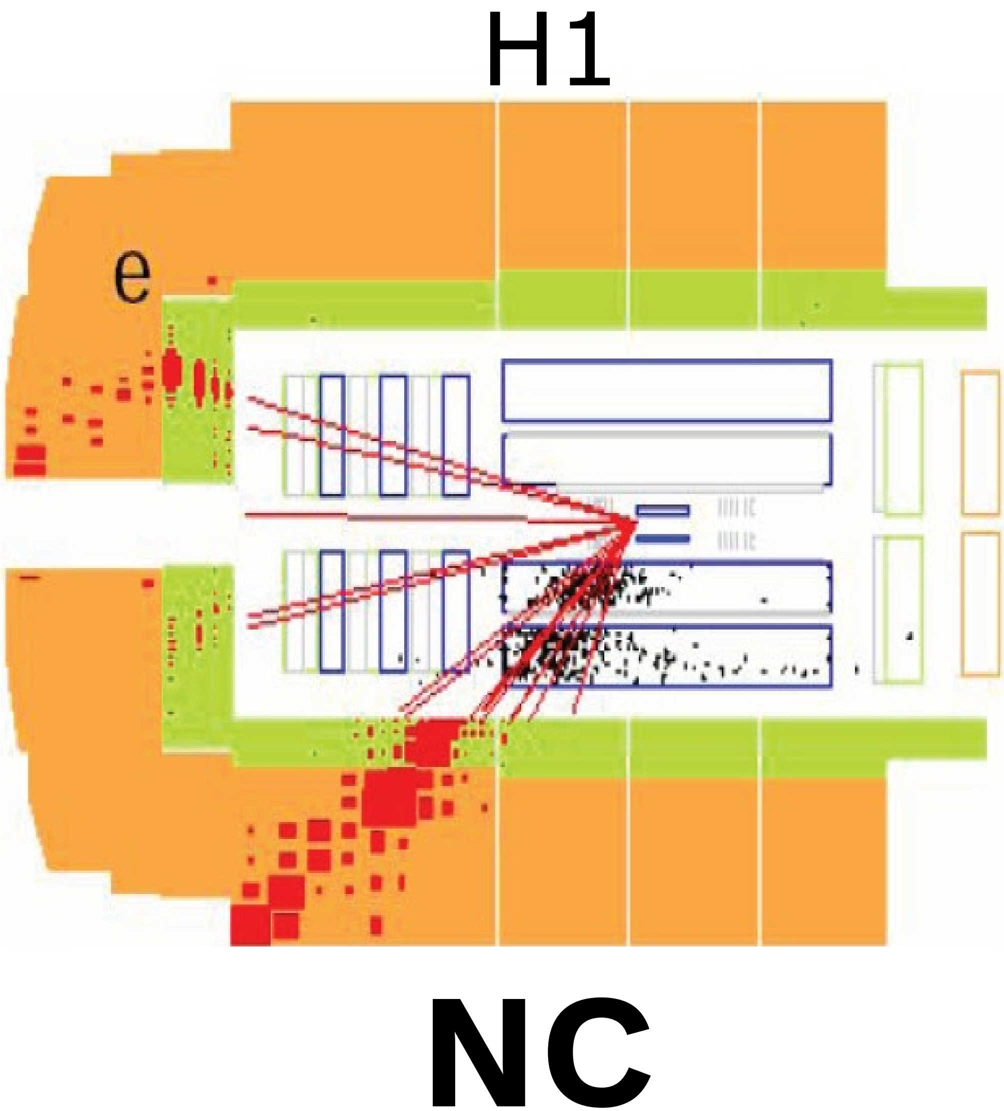


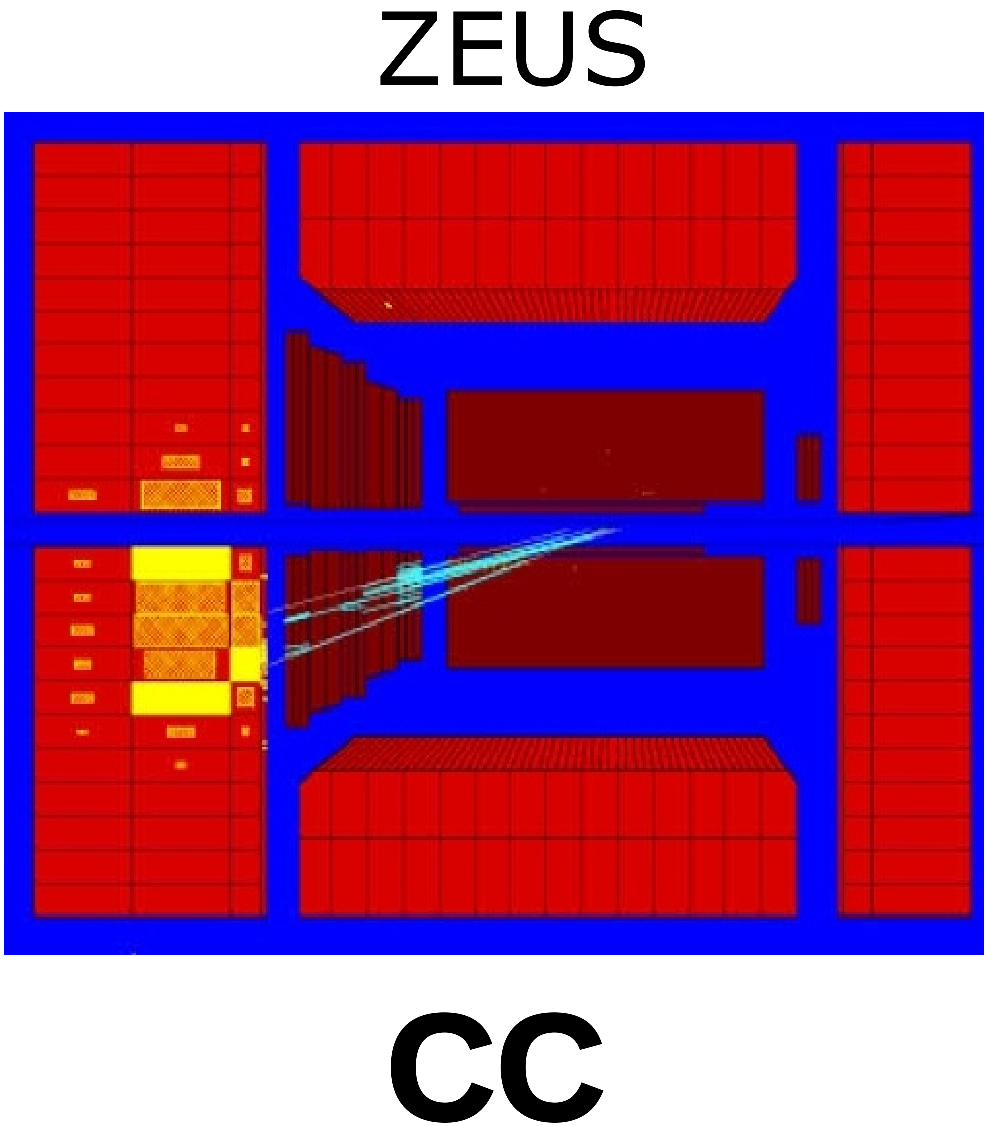

# DIS Cross Sections

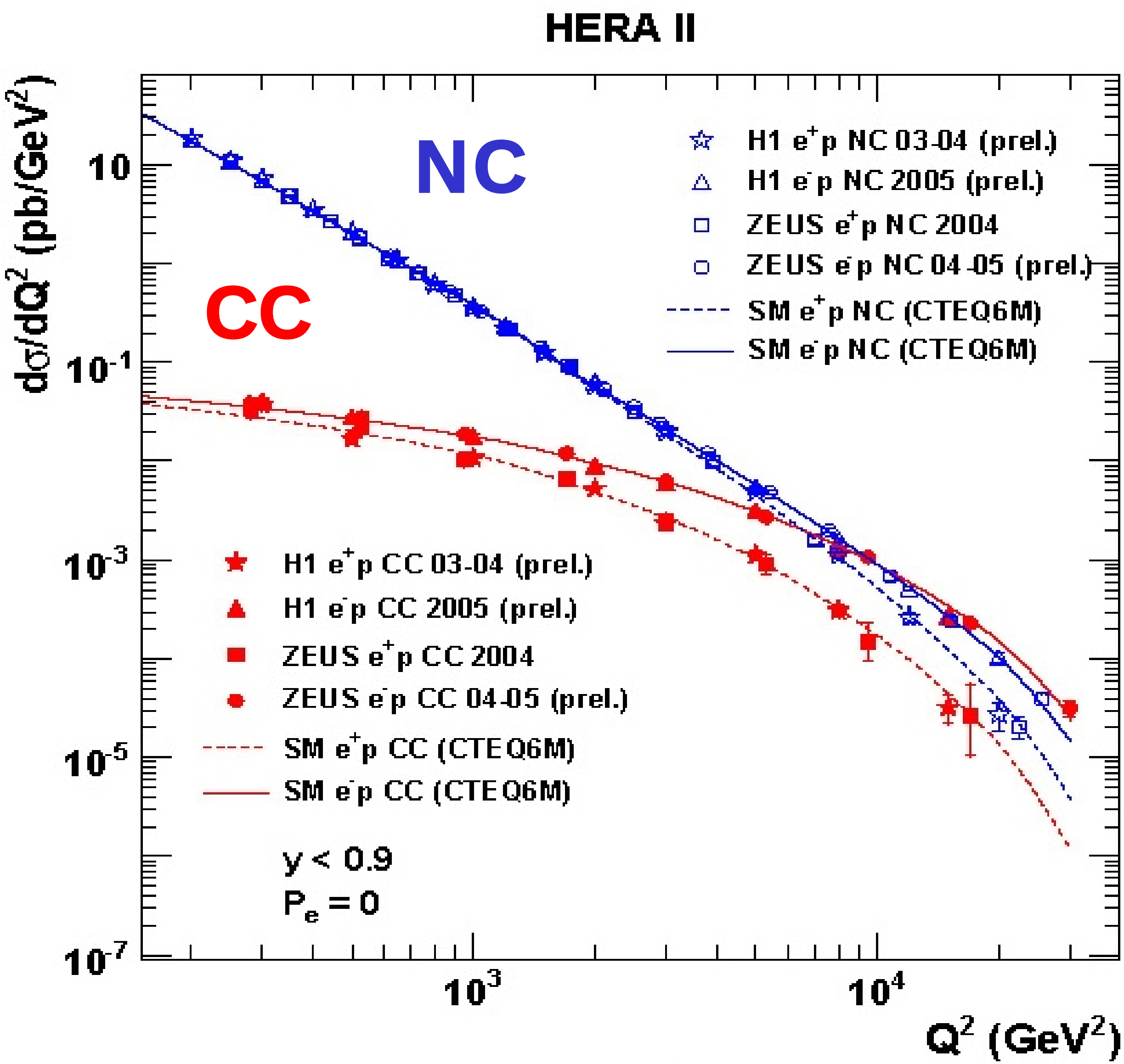


**ElectroWeak Unification**

when $Q^2 \approx M_W^2(M_Z^2)$

- NC dominated by $\gamma$ exchange (EM)
- $M_Z$ contributions (weak) at high $Q^2$
- CC cross sections (weak) become similar to NC at high $Q^2$
- $e^+/e^-$ differences at high $Q^2$
- Standard model holds up to the EW scale

# NC Cross Sections

Neutral Current (NC) $e^{\pm}p \rightarrow e^{\pm}X$ cross sections:

$$\frac{d^2\sigma(e^{\pm})}{dxdQ^2} = \frac{2\pi\alpha^2}{xQ^4}[Y_+ F_2(x,Q^2) - y^2 F_L(x,Q^2) \mp Y_- xF_3(x,Q^2)]$$

where $Y_{\pm} = 1 \pm (1-y)^2$

In the Quark-Parton Model representation, one would have from the quark and anti-quark densities:

$$F_2 = x\sum_q A_f(Q^2)[q(x,Q^2) + \bar{q}(x,Q^2)]$$

$$F_3 = x\sum_q B_f(Q^2)[q(x,Q^2) - \bar{q}(x,Q^2)]$$

$$F_L = F_2 - 2xF_1 = 0$$

with $F_2$ as the main term, parity-violating term $xF_3 \sim 0$ ( when $Q^2 << M_Z^2$)

and $F_L = 0$ for spin ½ partons (Callan-Gross relation). $F_L$ could become non-zero due to contributions from gluon radiation, hence measurable from data taken at different *ep* center-of-mass energies.

# $F_2$ Measurement

Large sets of measurements: pQCD proven valid down to **x**$\sim 10^{-4}$ and **$Q^2$**$\sim 1$ GeV$^2$

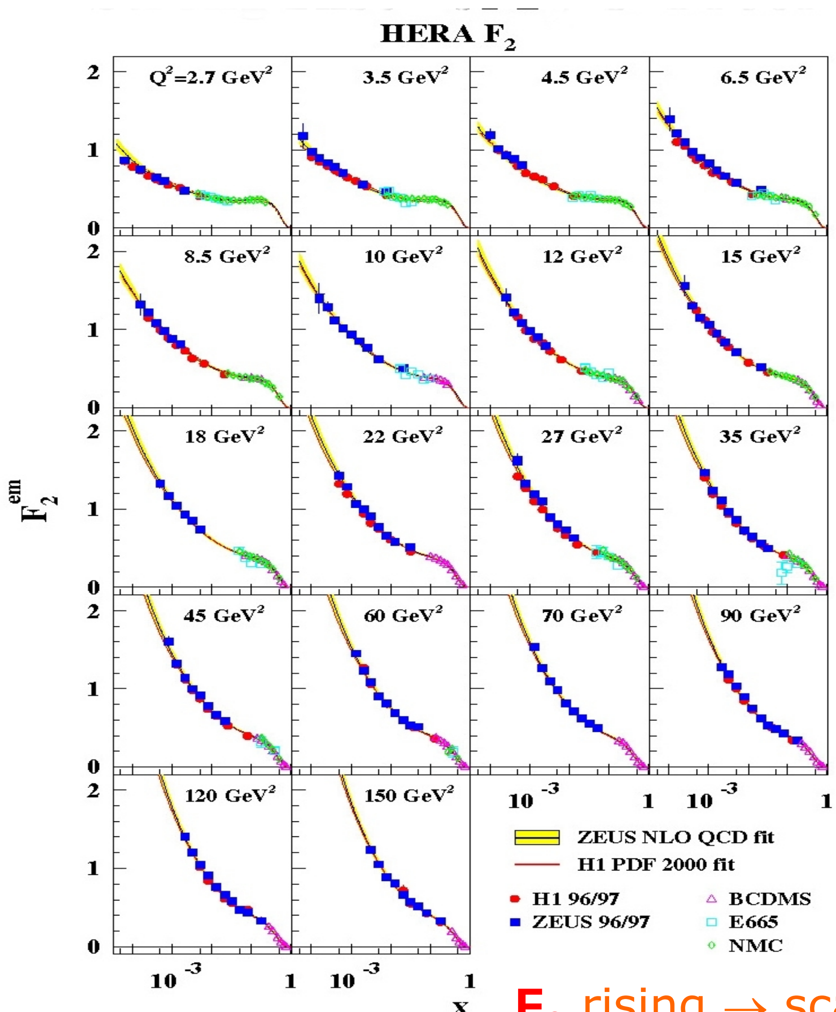


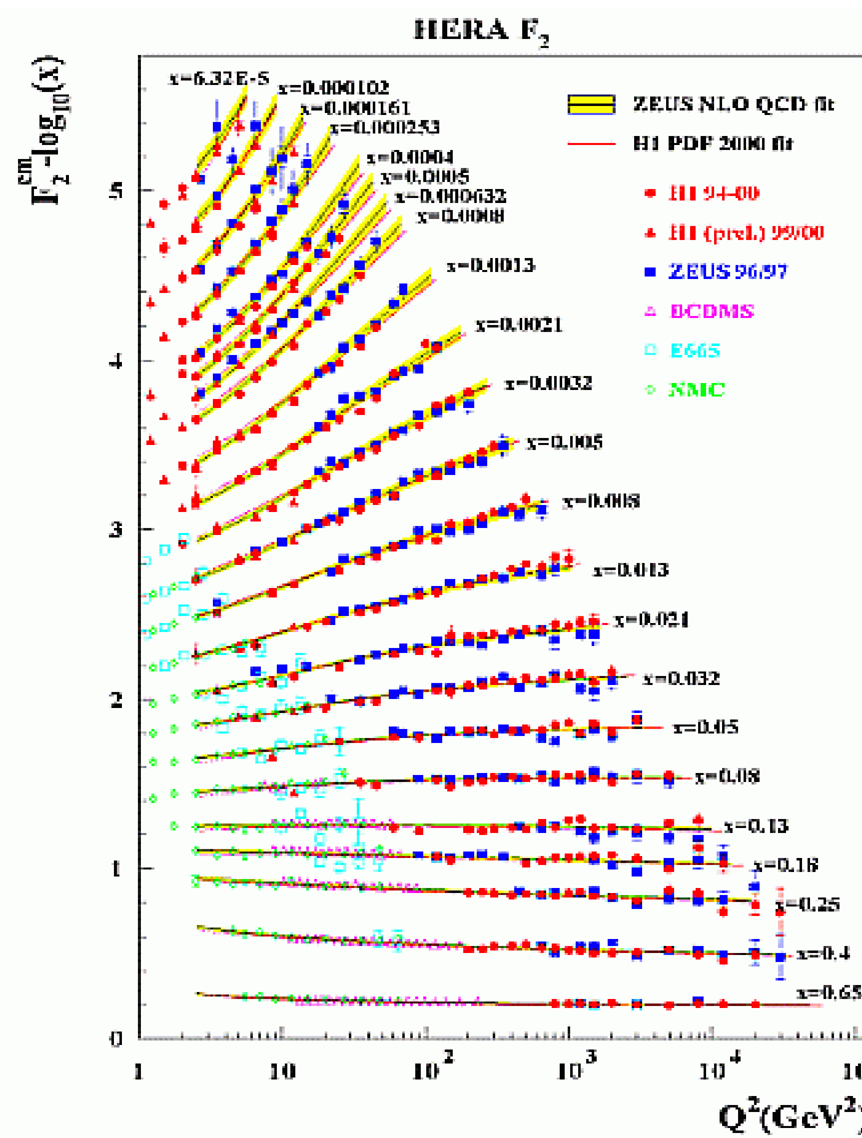


**$F_2$** rising → scaling violation → gluon density distributions

# Parton Density Functions

**HERA I**

**QCD next-to-leading order (NLO) fit analysis:**

~1500 data points from 14 experiments

+

statistical uncertainties, covariance matrices, estimated theory errors

=

parton momentum distributions for **u** and **d** valence quarks, sea quarks and gluons

+

$\alpha_s = 0.118 \pm 0.003$

(PDG: 0.1176±0.0009)

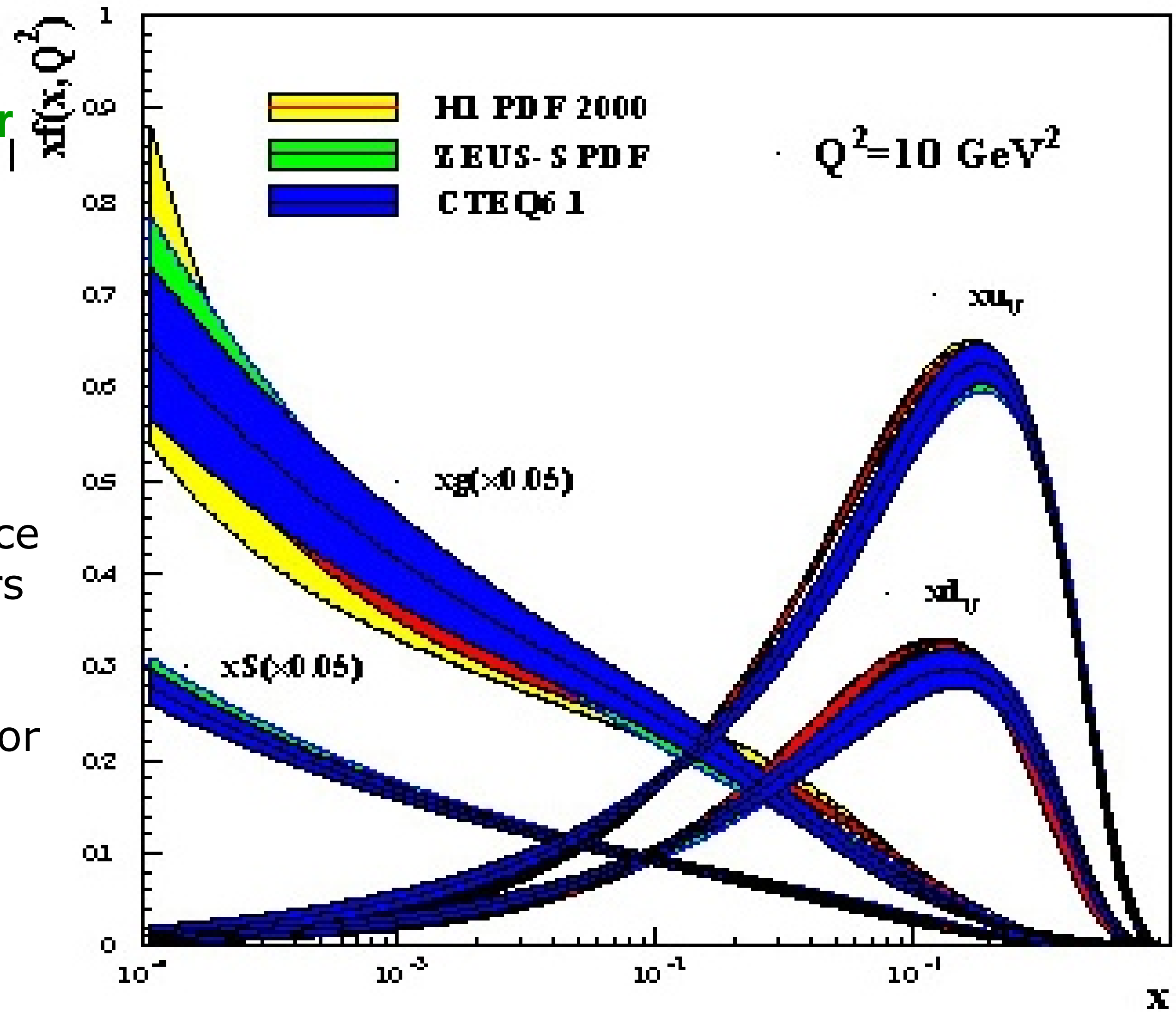

# $xF_3$ Extraction

## Use the DIS NC data with $e^+$ and $e^-$

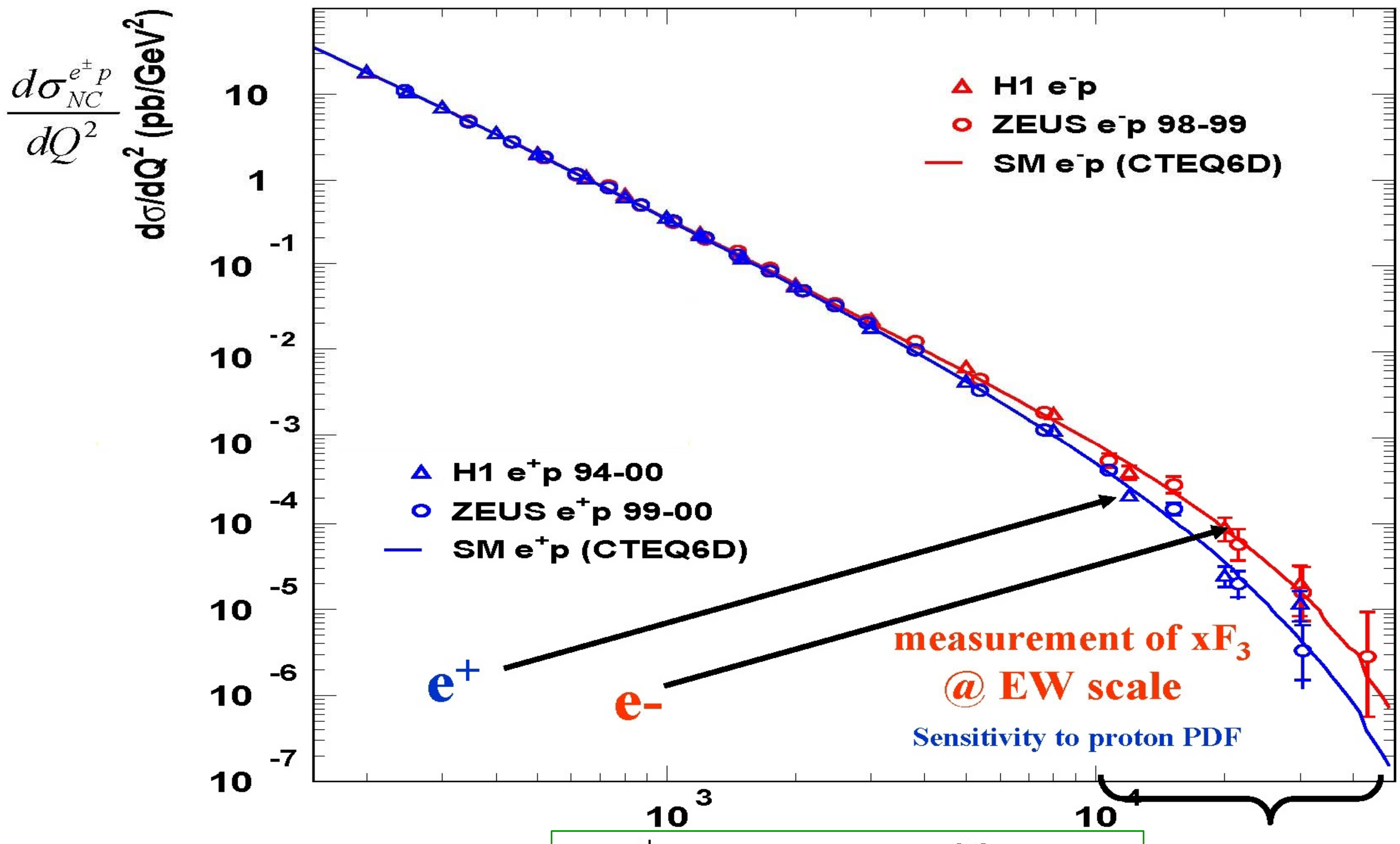


Reduced cross sections:

$$\tilde{\sigma}^{e^\pm p} = F_2 \mp \frac{Y_-}{Y_+} xF_3$$

# $xF_3^{\gamma Z}$ Extraction

$$xF_3 = -a_e \chi_Z xF_3^{\gamma Z} + 2 v_e a_e \chi_Z^2 xF_3^Z$$

**whereby $v_e$ is small and $\chi_Z<1$**

**When the analysis is redone for each x-bin, the interference structure function $xF_3^{\gamma Z}$ can be extracted:**

$$xF_3^{\gamma Z} \approx \frac{x}{3}(2u_v + d_v)$$

(+ small sea terms)

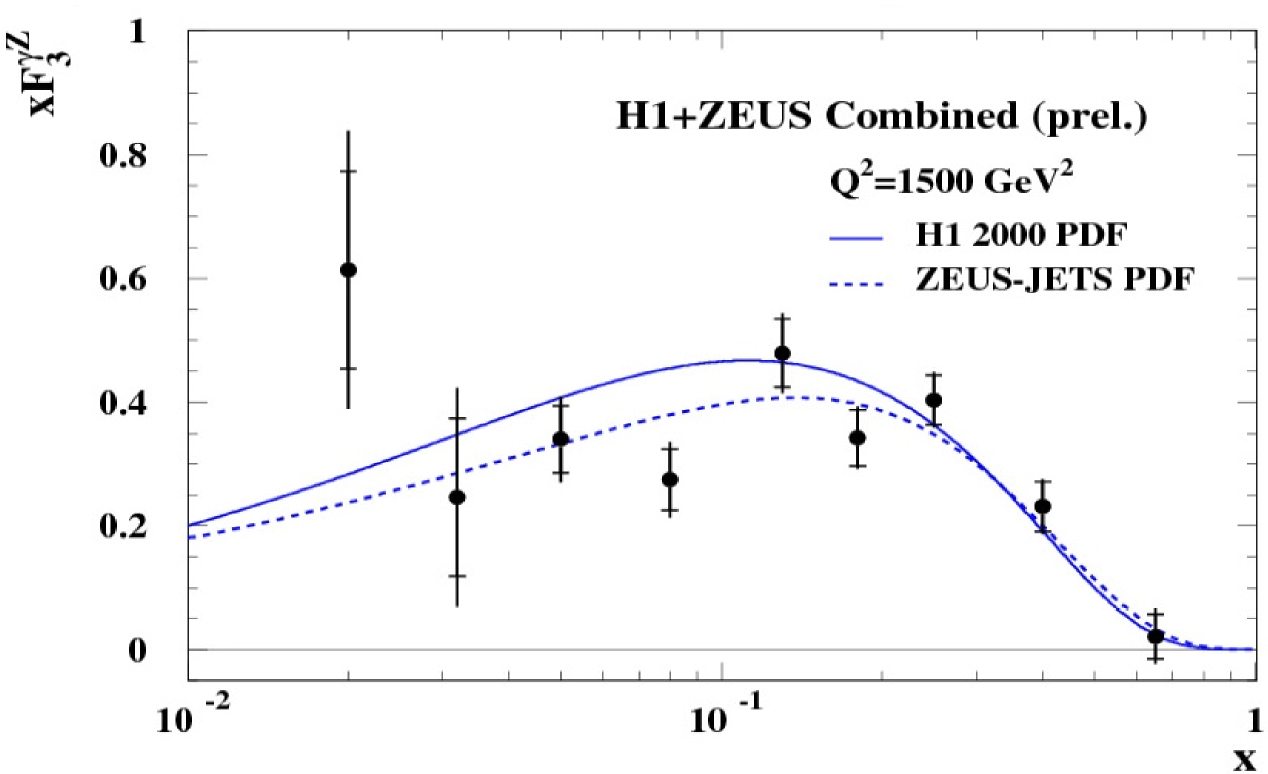


## The sum rules can be tested:

$$\int_0^1 F_3^{\gamma Z} dx = \int_0^1 (\tfrac{2}{3}u_v + \tfrac{1}{3}d_v) dx = \tfrac{5}{3}$$

**H1+ZEUS:**

$$\int_{0.02}^{0.65} F_3^{\gamma Z} dx = 1.21 \pm 0.09(\mathrm{stat}) \pm 0.08(\mathrm{sys})$$

**H1 QCD fits:**

$$\int_{0.02}^{0.65} F_3^{\gamma Z} dx = 1.12 \pm 0.02$$

**ZEUS QCD fits:**

$$\int_{0.02}^{0.65} F_3^{\gamma Z} dx = 1.06 \pm 0.02$$

# e± Polarisation

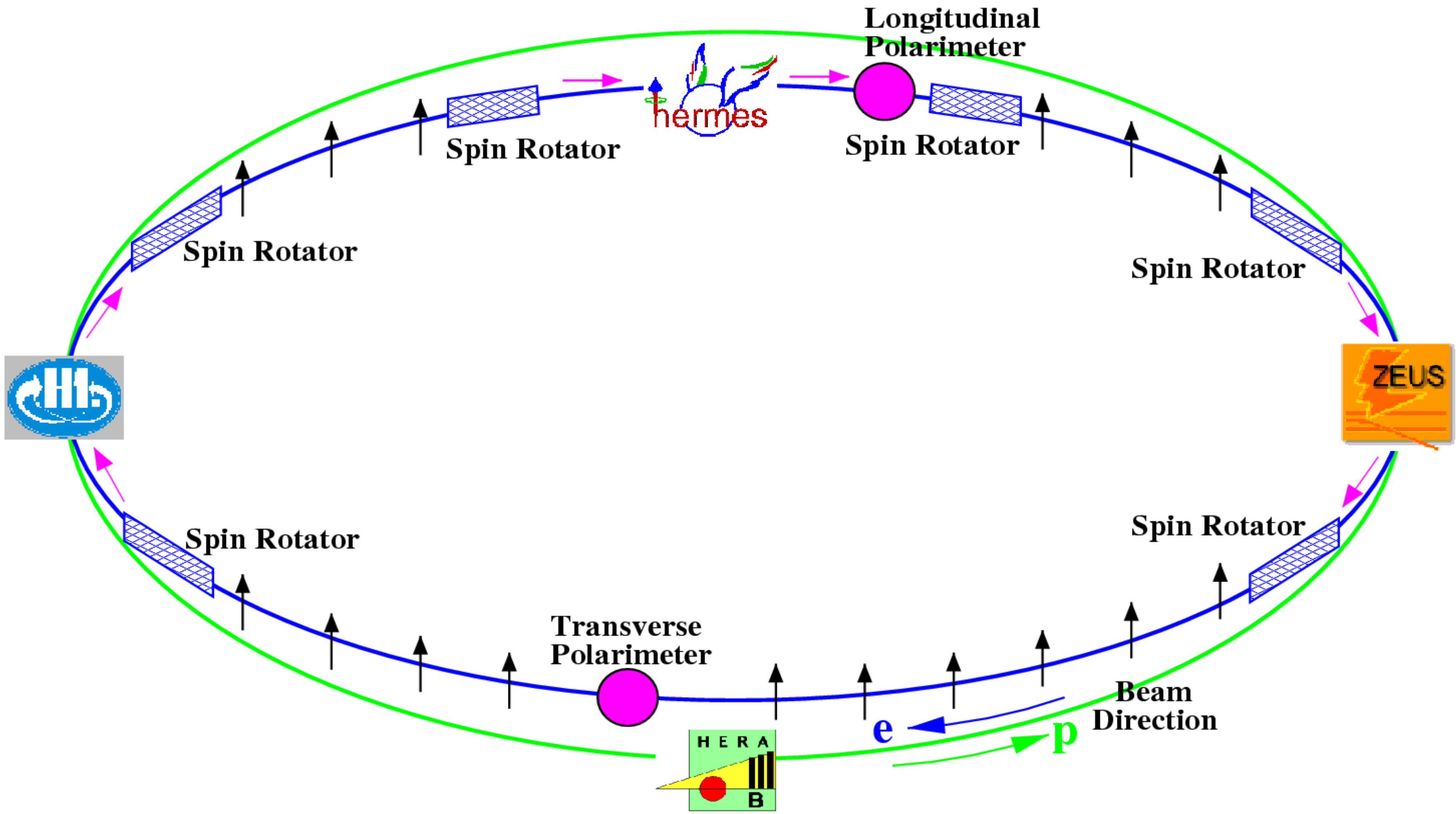


**LPOL** measures the longitudinal polarisation at HERMES

**TPOL** measures the transverse polarisation between ZEUS and H1

# HERA Luminosities

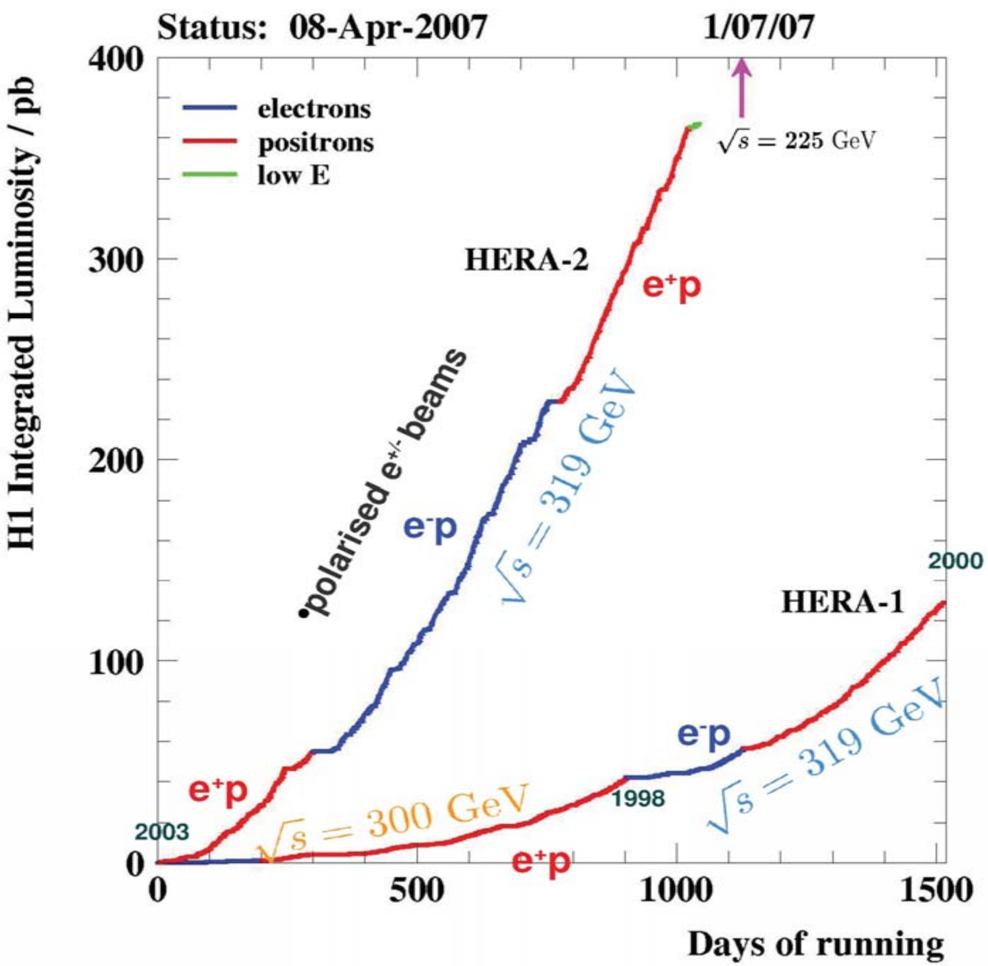


gated ≈ 0.5 $fb^{-1}$ per experiment

**HERA I: unpolarised $e^{\pm}$ beams**

**HERA II: polarised $e^{\pm}$ beams**

## Delivered luminosities:

| | | $E_e$ | $E_p$ | $e^+p$ | $e^-p$ |
|---|---|---|---|---|---|
| **HERA I** | HER | 27.6 GeV | 820/ 920 | 165 $pb^{-1}$ | 27 $pb^{-1}$ |
| **HERA II** | HER | 27.6 GeV | 920 GeV | 270 $pb^{-1}$ | 290 $pb^{-1}$ |
| | LER | 27.6 GeV | 460 GeV | 15 $pb^{-1}$ | |
| | MER | 27.6 GeV | 575 GeV | 9 $pb^{-1}$ | |

(approximate figures)

# NC – Parity Violation

Calculate asymmetry between L/R-handed cross sections:
**parity violation** due to $\gamma Z$ interference ($a_e v_q$ term):

$$\tilde{\sigma}(e_L^- p) - \tilde{\sigma}(e_R^- p) \sim 2F_2^P \simeq 2\sum(q+\bar{q})2e_q a_e v_q \chi_Z$$

$$(\chi_Z = \frac{Q^2}{Q^2+M_Z^2}\frac{1}{\sin^2 2\theta_W})$$

**combine e$^+$ and e$^-$ data**

$$A^{\pm} = \frac{2}{P_e^+ - P_e^-} \cdot \frac{\sigma^{\pm}(P_e^+) - \sigma^{\pm}(P_e^-)}{\sigma^{\pm}(P_e^+) + \sigma^{\pm}(P_e^-)} \approx \mp \chi_z a_e \frac{F_2^{\gamma Z}}{F_2^{\gamma}}$$

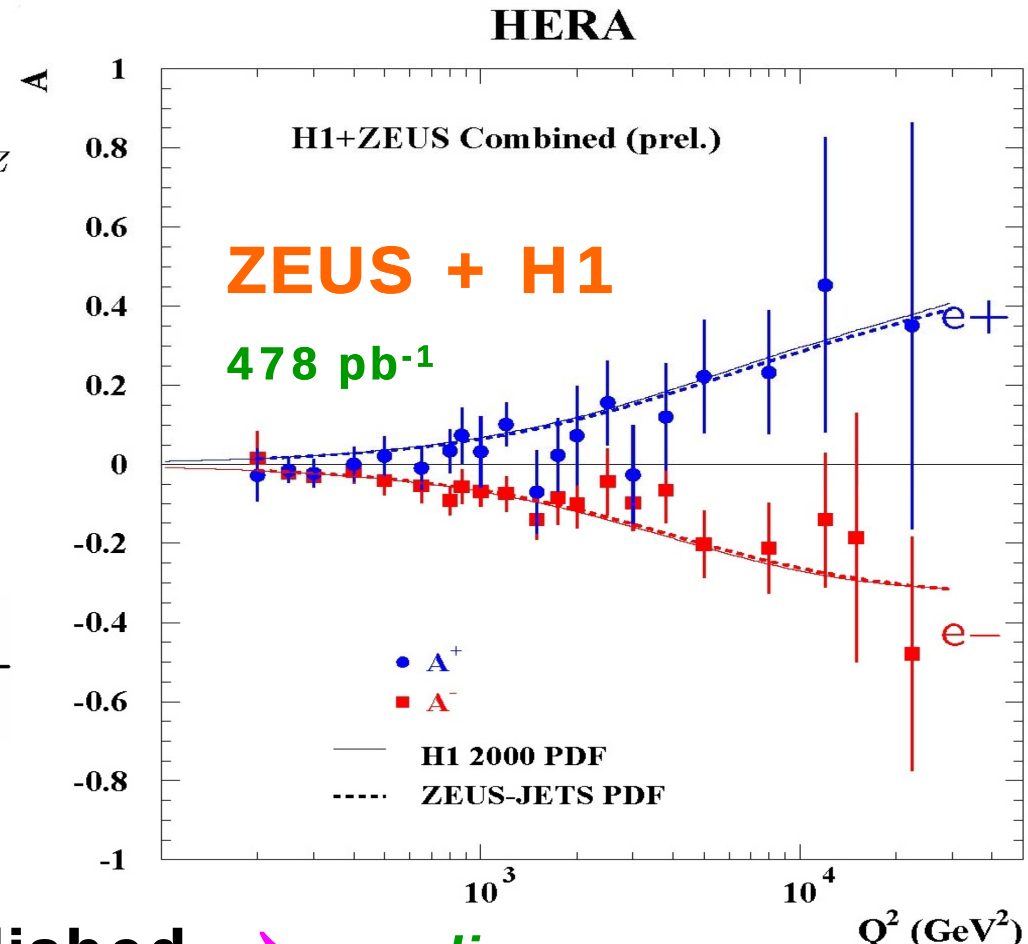


**Parity violation clearly established → *couplings***

# NC - Couplings

## Light quark coupling to Z

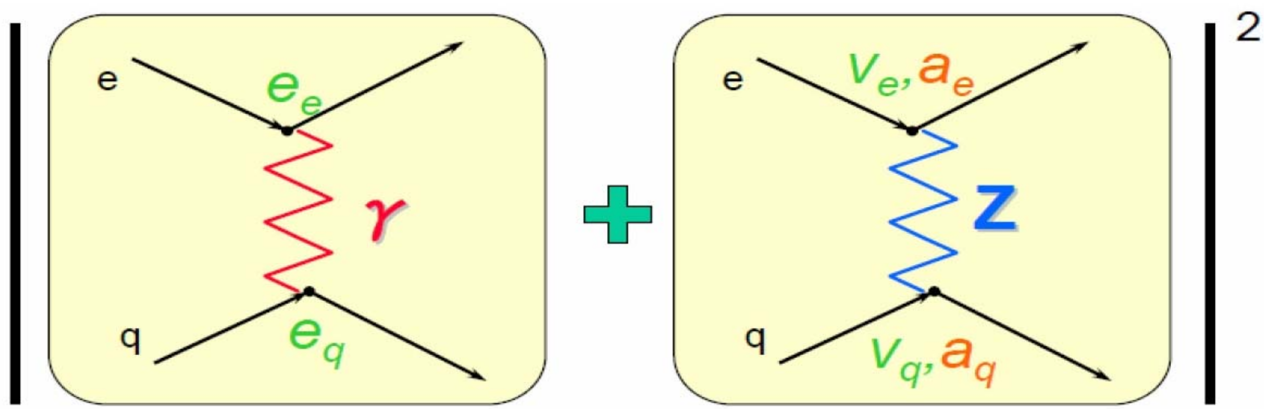


"known" SM coupling strengths

| | v | a |
|---|---|---|
| e | -0.04 | -0.5 |
| u | 0.196 | 0.5 |
| d | -0.346 | -0.5 |

$$\tilde{F}_2 = F_2^{\gamma} - (v_e \pm P_e a_e)\chi_Z F_2^{\gamma Z} + ((v_e^2 + a_e^2) \pm P_e 2 v_e a_e))\chi_Z^2 F_2^Z$$
$$\tilde{F}_3 = - (a_e \pm P_e v_e)\chi_Z F_3^{\gamma Z} + ((2 v_e a_e \pm P_e (v_e^2 + a_e^2))\chi_Z^2 F_3^Z$$

*i.e. 4 new EW structure functions accessible*

$$\chi_Z = \frac{1}{\sin^2 2\theta_w}\left(\frac{Q^2}{Q^2 + M_Z^2}\right)$$

Unpolarised data: $\sigma(e^+) - \sigma(e^-) \rightarrow F_3^{\gamma Z} \rightarrow a_e$ (as before, assuming $v_e$ small)

Polarised data: $\sigma(+P_e) - \sigma(-P_e) \rightarrow F_2^{\gamma Z} \rightarrow v_e$

.. work to be followed

# EW Couplings for *u* and *d* quarks

In the quark-parton model, one has:

$$F_2^{\gamma Z} = 2e_f v_f \Sigma_i x[q_f + \overline{q_f}]$$
$$F_2^{Z} = (v_f^2 + a_f^2)\Sigma_i x[q_f + \overline{q_f}]$$
$$F_3^{\gamma Z} = 2e_f a_f \Sigma_i x[q_f - \overline{q_f}]$$
$$F_3^{Z} = 2v_f a_f \Sigma_i x[q_f - \overline{q_f}]$$

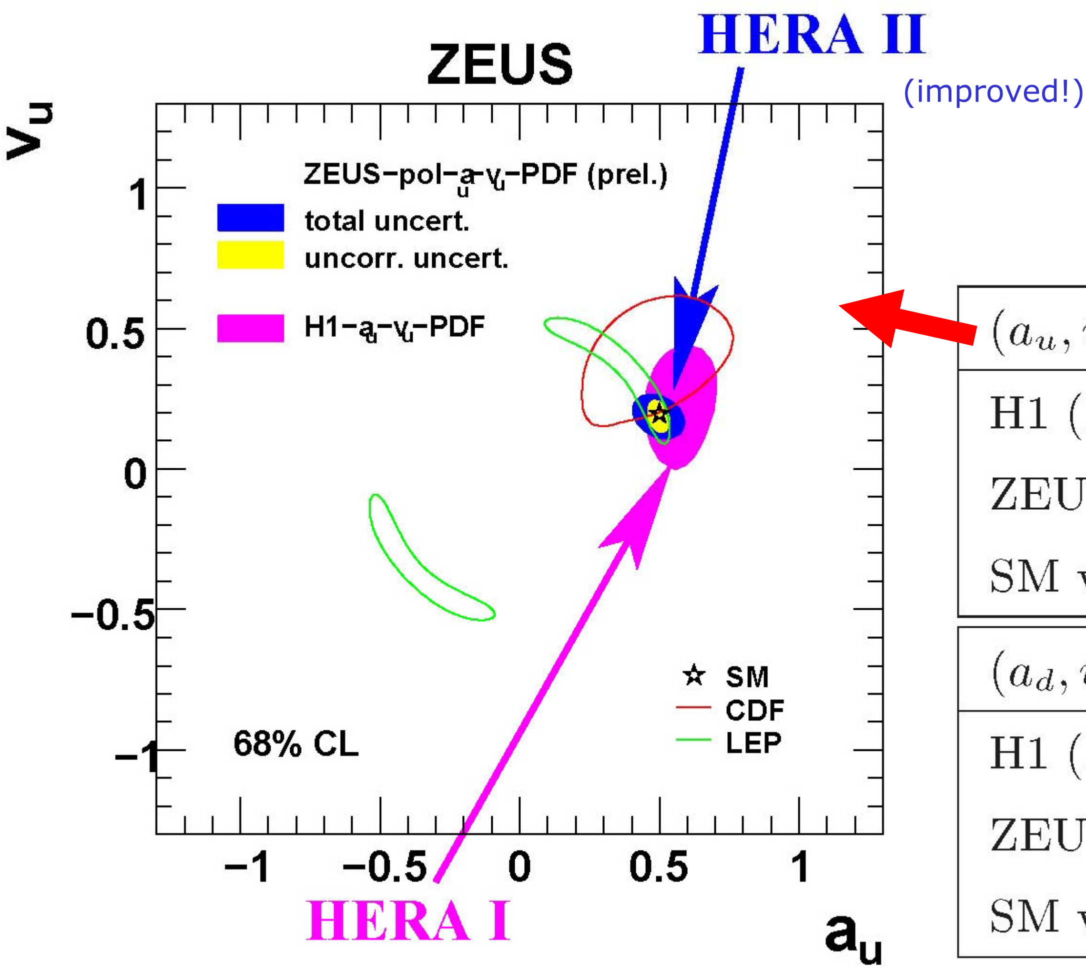


| $(a_u, v_u)$ Fit | $a_u$ | $v_u$ |
|---|---|---|
| H1 (HERA I) | $0.57 \pm 0.08$ | $0.27 \pm 0.13$ |
| ZEUS (HERA II) | $0.50 \pm 0.10$ | $0.19 \pm 0.08$ |
| SM value | 0.5 | 0.196 |

| $(a_d, v_d)$ Fit | $a_d$ | $v_d$ |
|---|---|---|
| H1 (HERA I) | $-0.80 \pm 0.24$ | $-0.33 \pm 0.33$ |
| ZEUS (HERA II) | $-0.49 \pm 0.30$ | $-0.37 \pm 0.22$ |
| SM value | -0.5 | -0.346 |

# Couplings to Z: NC/CC Data Fit

Ongoing analysis results with part of the HERA II data:

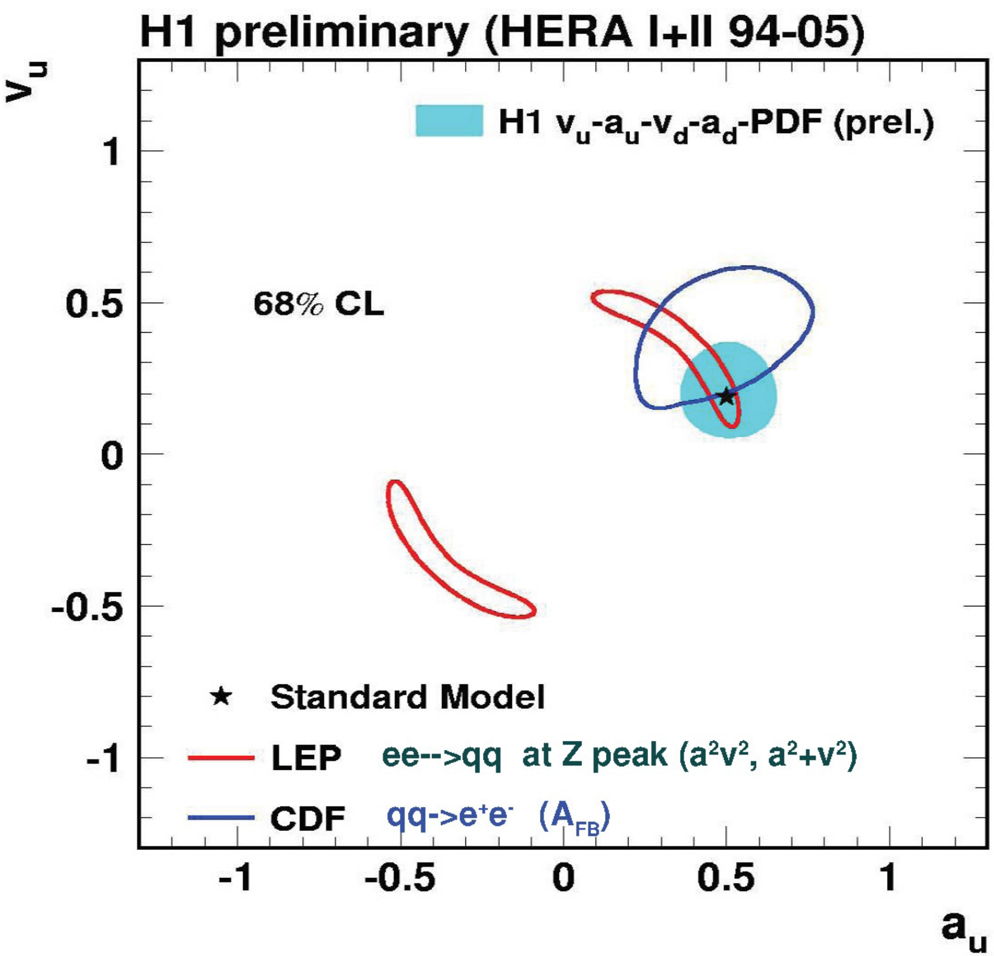


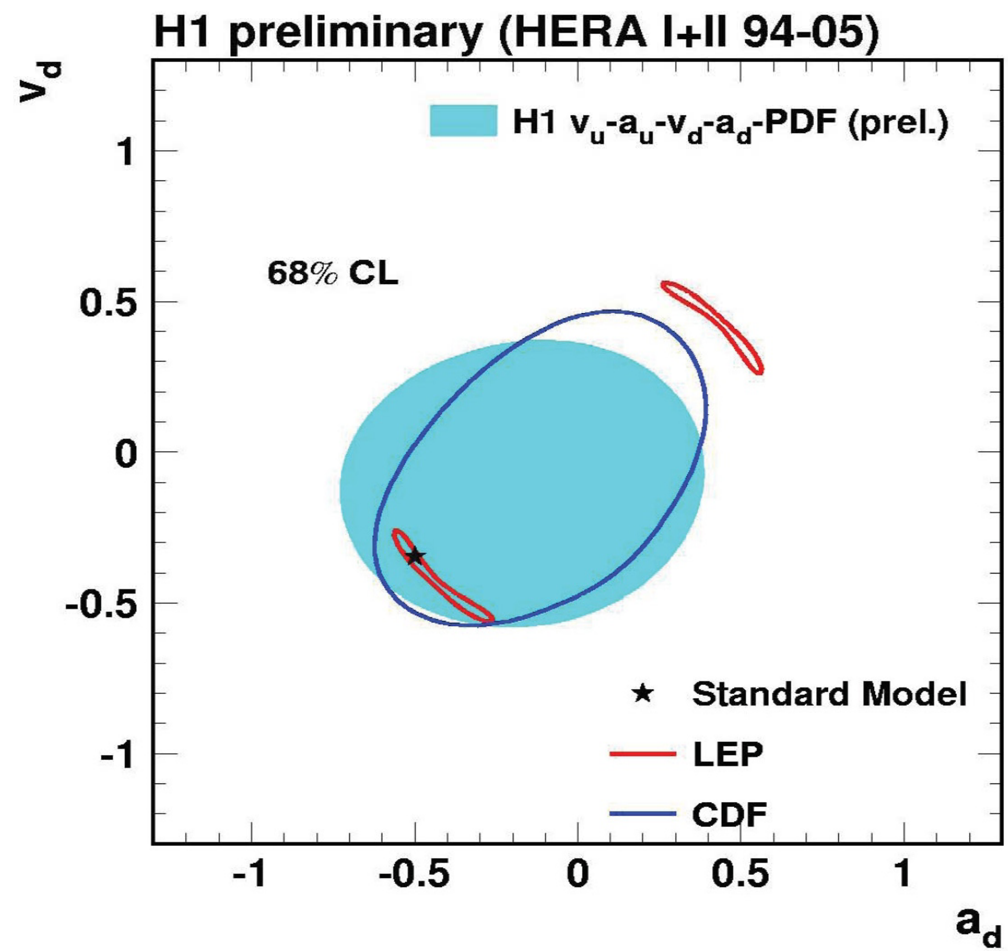

# CC – Helicity Dependence

$$\sigma_{CC}^{e^\pm p}(P) = (1 \pm P) \cdot \sigma_{CC}^{e^\pm p}(0)$$

As expected, strong linear dependence on polarisation

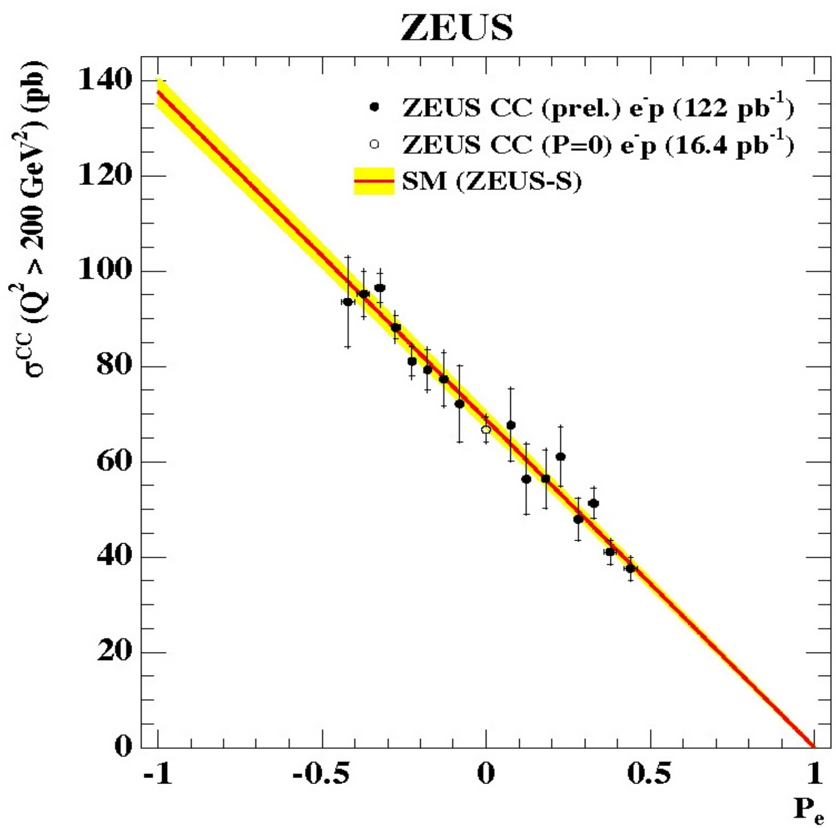


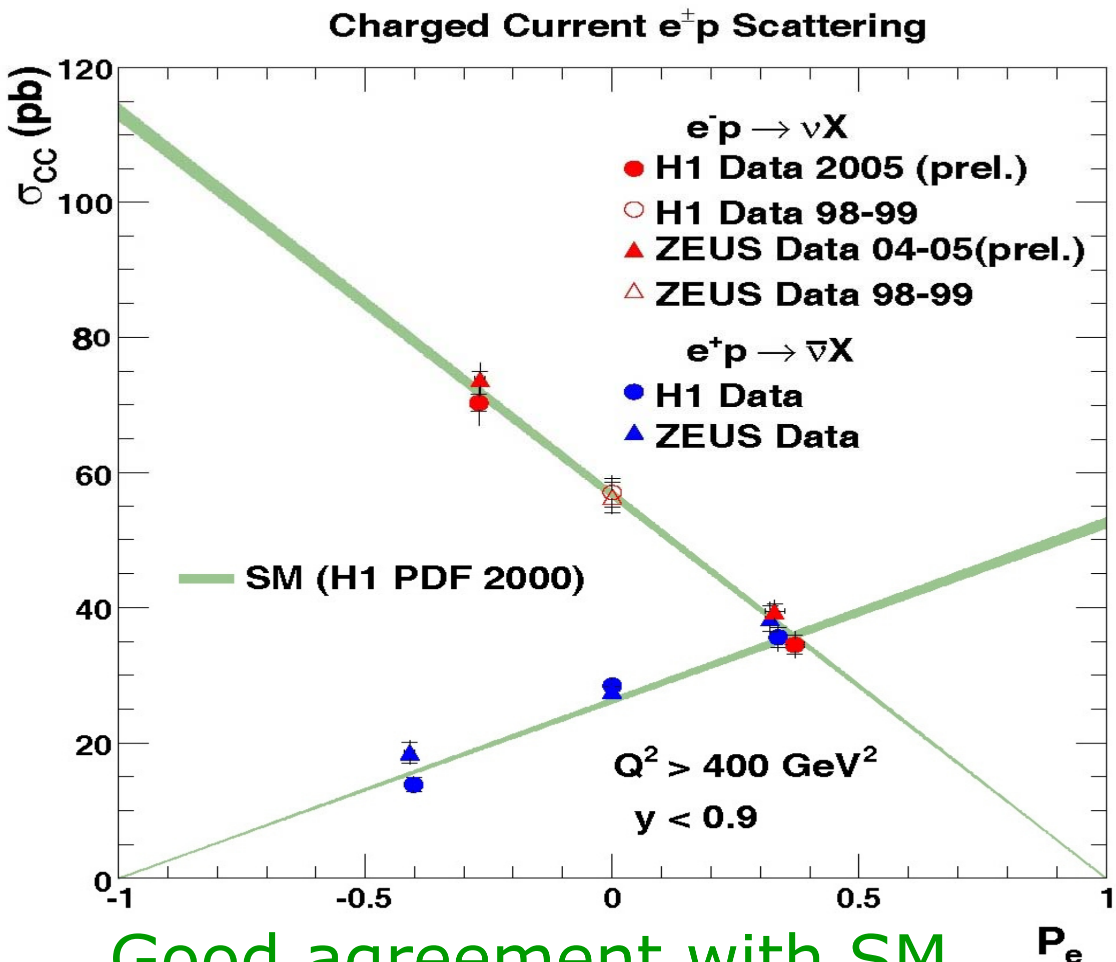


Good agreement with SM

$\sigma(e^-)$ extrapolated to $P_e=1$ →

**ZEUS:** 0.8 pb ± 3.1(stat) ± 5.0(syst+pol)
**H1:** -0.9 pb ± 2.9(stat) ± 1.9(syst) ± 2.9(pol)

# CC – $W_R$ Mass Limit

## (Ongoing) Search for right-handed currents

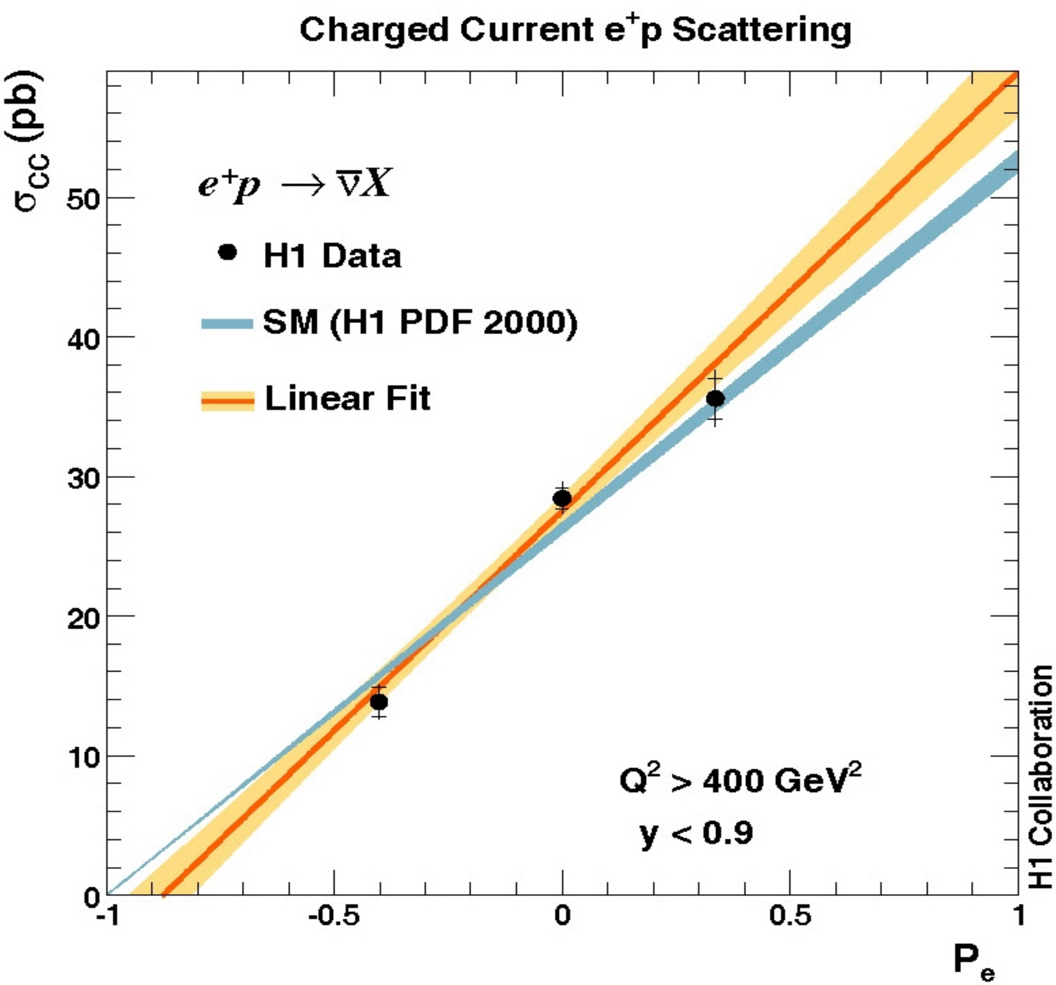


$e^+p \rightarrow \nu X$

Assuming $g_L = g_R$ and $\nu_R$ light:

**M($W_R$) > 208 GeV (H1 $e^+$)**

(errors dominated by the polarisation uncertainty)

Similar prelim. results from ZEUS

polarised $^{12}$N decay: > 310 GeV

# $F_L$ Extraction

**Reminder:**

$$\frac{d^2\sigma_{NC}(e^\pm p)}{dxdQ^2} = \frac{2\pi\alpha^2}{xQ^4}[Y_+F_2 \mp Y_-xF_3 - y^2F_L]$$

**and (from the electron):**

$$y = 1 - \frac{E'_e}{2E_e}(1 - \cos\theta_e)$$

**$F_L$** explores the small-**x** physics and the gluon densities distributions where the theoretical uncertainties run from large to very large.

**Extraction:**

$$F_L(x,Q^2) = \frac{\tilde{\sigma}_1(x,Q^2,y_1) - \tilde{\sigma}_2(x,Q^2,y_2)}{\frac{y_2^2}{Y_{2+}} - \frac{y_1^2}{Y_{1+}}}$$

For fixed (**x**,**Q²**), measurements must be done at different **y** values. Low **proton** energy running (LER) leads to high **y** values, hence better level arm with nominal HER and more precise **$F_L$**

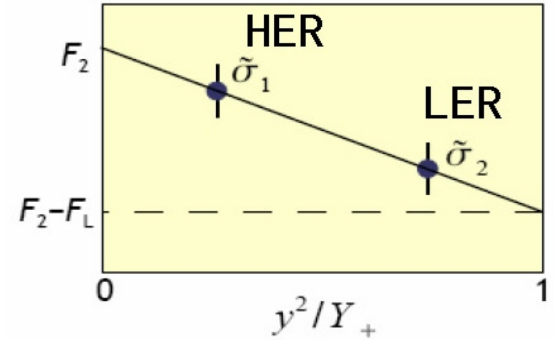

# Low Energy Running

$E_p$ = 460 GeV

a compromise between low $E_p$ and e-p luminosity

e+/p beams

specific luminosity

polarisation

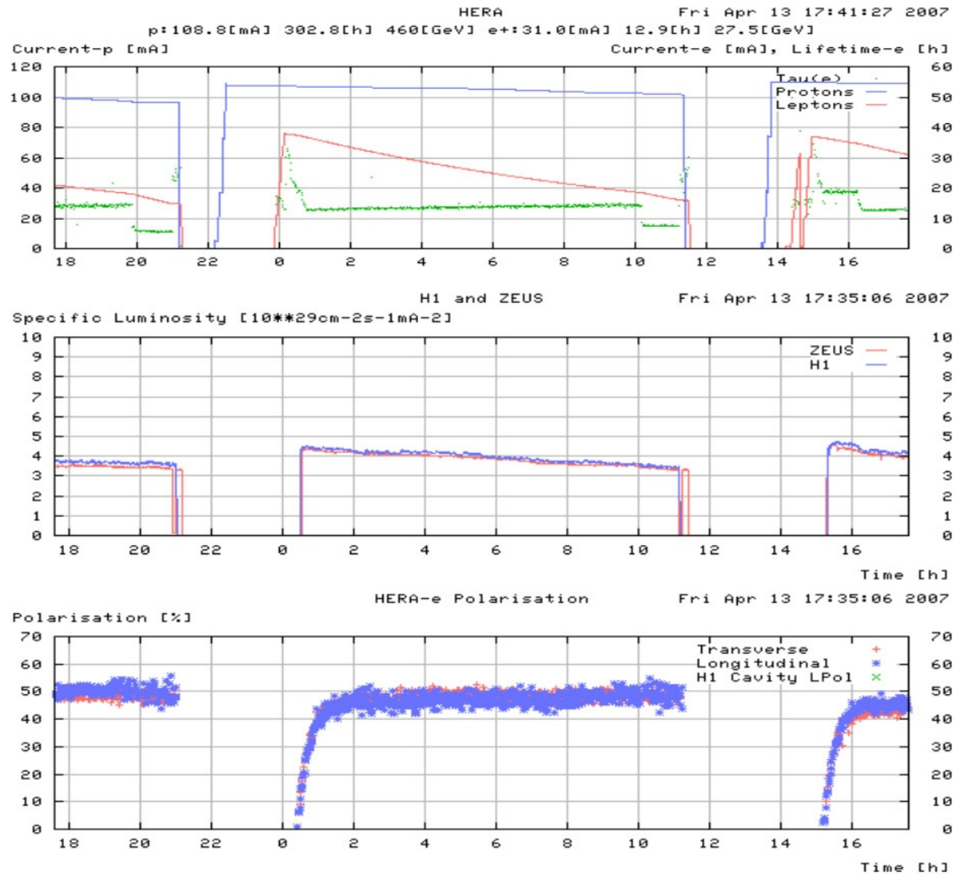


smooth transition

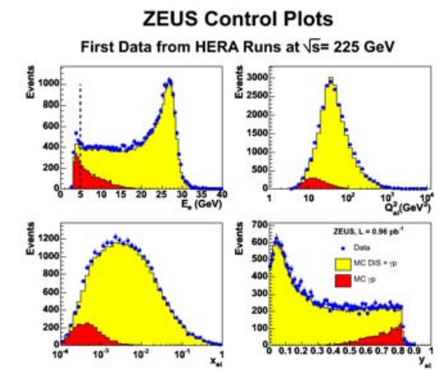


13 $pb^{-1}$ collected

$E_p$ = 575 GeV

from June 11th until the end of HERA

8 $pb^{-1}$

**.. stay tuned, physics data to be analysed!**

# Quark Radius

Comparisons with the Standard Model as searches for new contributions: contact interactions (Λ up to 7.5 TeV), large extra dimensions, quark structure, ..

The form factor **$R_q$** corresponds to the average radius of the quark charge which would modify the SM DIS cross sections:

$$\frac{d\sigma}{dQ^2} = \left(\frac{d\sigma}{dQ^2}\right)_{SM} \left(1 - \frac{1}{6} R_q^2 Q^2\right)^2$$

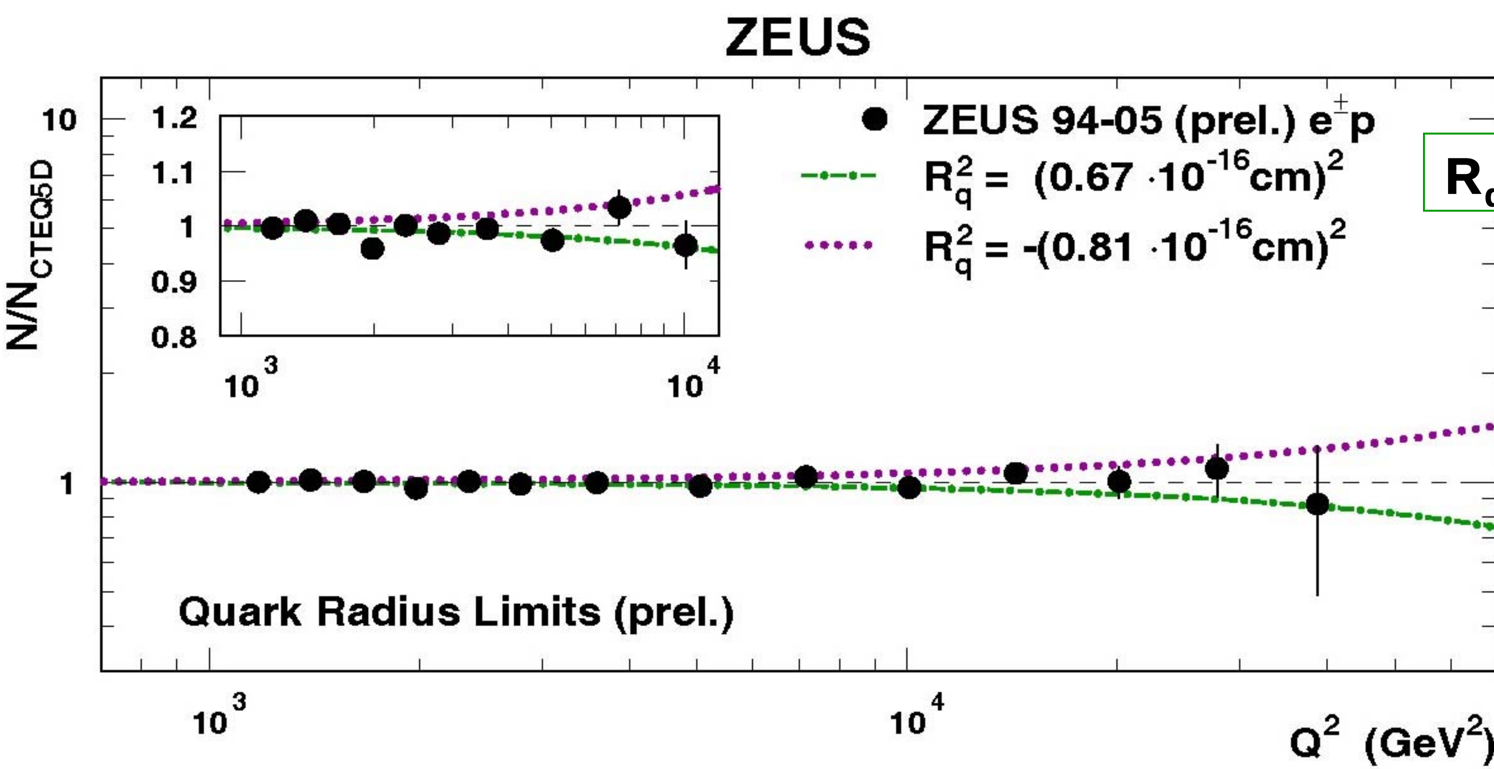


**$R_q < 0.67 \cdot 10^{-3}$ fm !**

# High $p_T$ Leptons

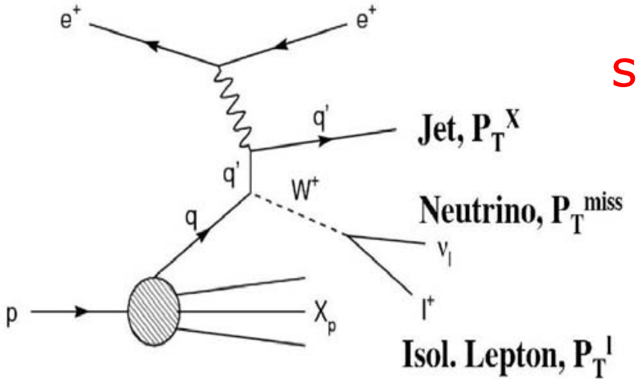


single W production → isolated lepton ($\sigma$~1.1 pb at HERA)

+ large missing $p_T$ (look for $p_T^X$>25 GeV)

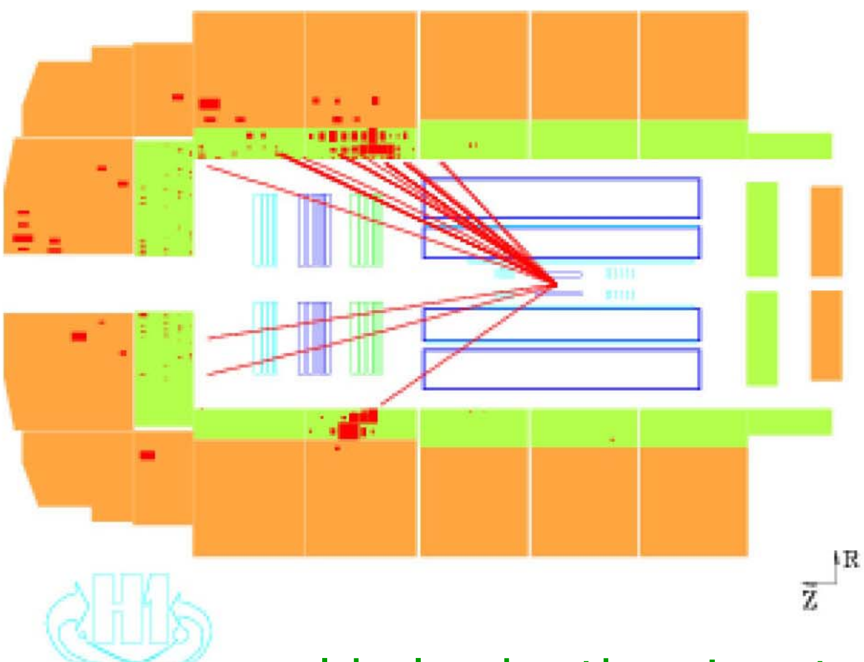


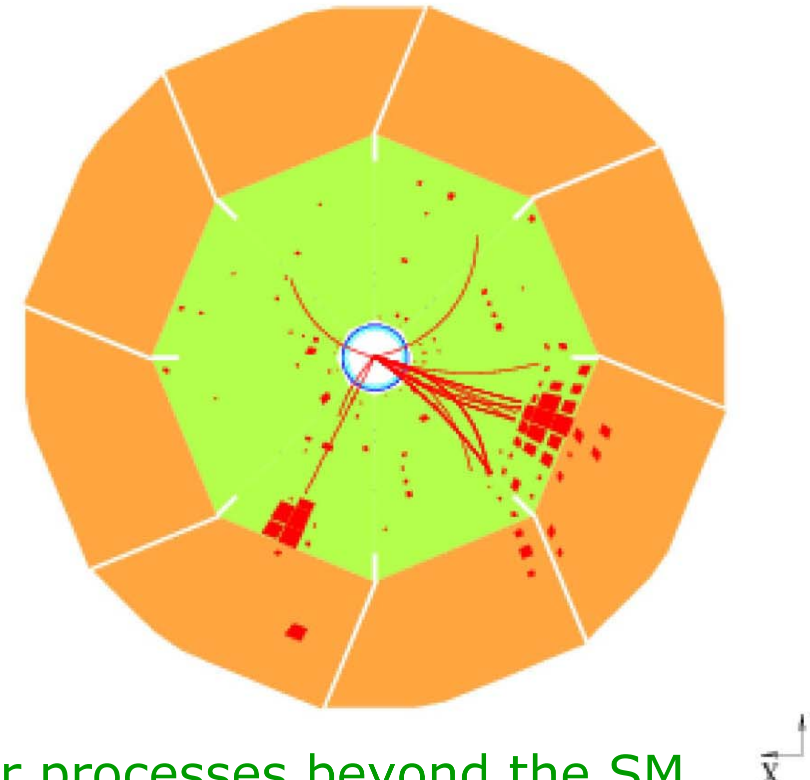


.. could also be the signature for processes beyond the SM

# High $p_T$ Leptons

| | $P_T^X > 25$ GeV | | electrons data / SM | muons data / SM |
|---|---|---|---|---|
| e+ | H1 | 294 $pb^{-1}$ | 11 / 4.7 ± 0.9 | 10 / 4.2 ± 0.7 |
| | ZEUS | 228 $pb^{-1}$ | 1 / 3.2 ± 0.4 | 3 / 3.1 ± 0.5 |
| e- | H1 | 184 $pb^{-1}$ | 3 / 3.8 ± 0.6 | 0 / 3.1 ± 0.5 |
| | ZEUS | 204 $pb^{-1}$ | 5 / 3.8 ± 0.6 | 2 / 2.2 ± 0.3 |

general agreement with the SM, except for a 3σ effect in $e^+p$ for H1 only .. not clarified yet.

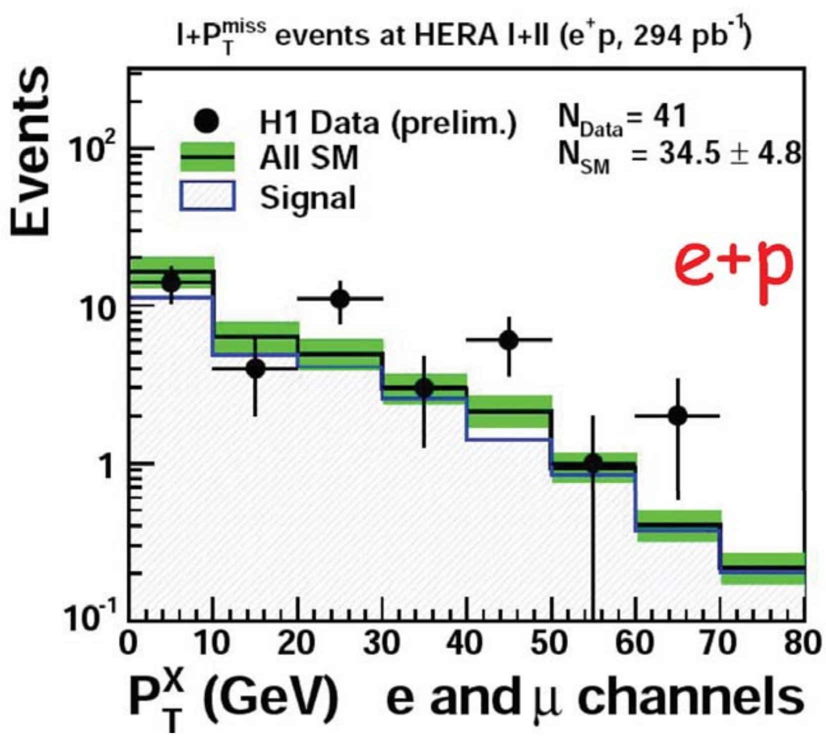


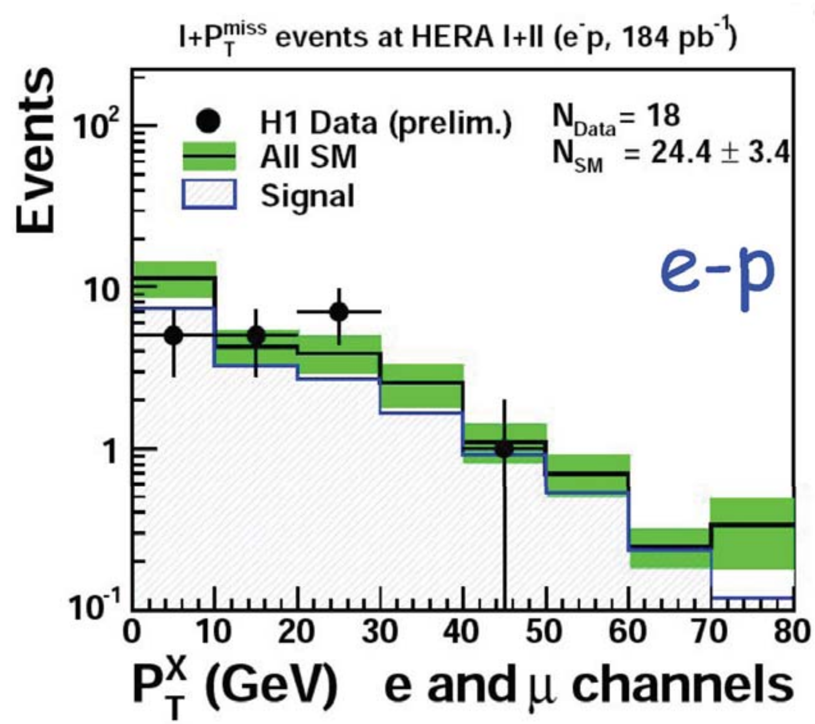


τ-channel also studied by H1 in CC events (larger backgrounds and lower efficiencies): **no excess observed**

# HERA - LHC

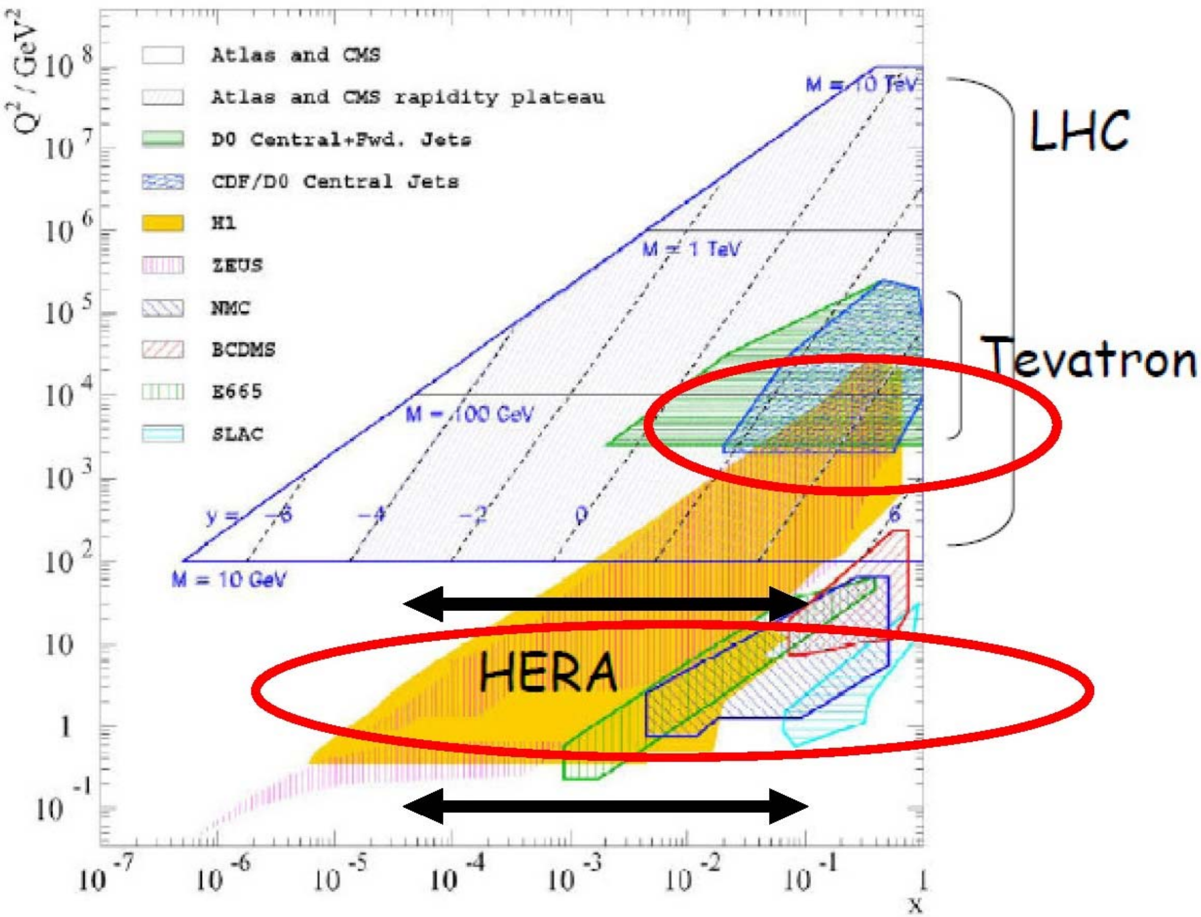



PDF and fragmentation data should have a large impact on LHC physics, in particular at low x values.

# Outlook

- After 23 years since conception, 15 years of operation, HERA stopped on June 30th, 2007. An integrated luminosity of 1 $fb^{-1}$ was taken by both experiments H1 and ZEUS combined.

- The HERA II program provided polarisation and high luminosity, thus enabling us to study EW physics at the EW scale (large $Q^2$'s) and deepen our understanding of the proton structure.

- There are still lots of other physics topics investigated, particularly in low x, QCD, diffraction, exotics and searches, etc.. HERA has a rich program that should be completed. Many more results to come!

of an Hera

# The End

# $M_W$ Determination

The mass of the W vector boson appears explicitely in the CC cross section expressions, e.g.:

**CC $e^+p$ cross section:**

$$\frac{d^2\sigma^{CC}(e^+p)}{dxdQ^2} = \frac{G_F^2}{4\pi x}\left(\frac{M_W^2}{M_W^2+Q^2}\right)^2\left[\bar{u}+\bar{c}+(1-y)^2(d+s)\right]$$

Assuming $G_F$ fixed (from muon decay), one gets:

$M_W$ = 80.3 ± 2.1 (stat) ± 1.2 (syst) ± 1.0 (PDF) GeV

**PDG**: $M_W$ = 80.403 ± 0.029 GeV

The observed precision may be large, but the results are fully complementary e.g. to LEP's and consistent!

# Inclusive Jets and $\alpha_s$

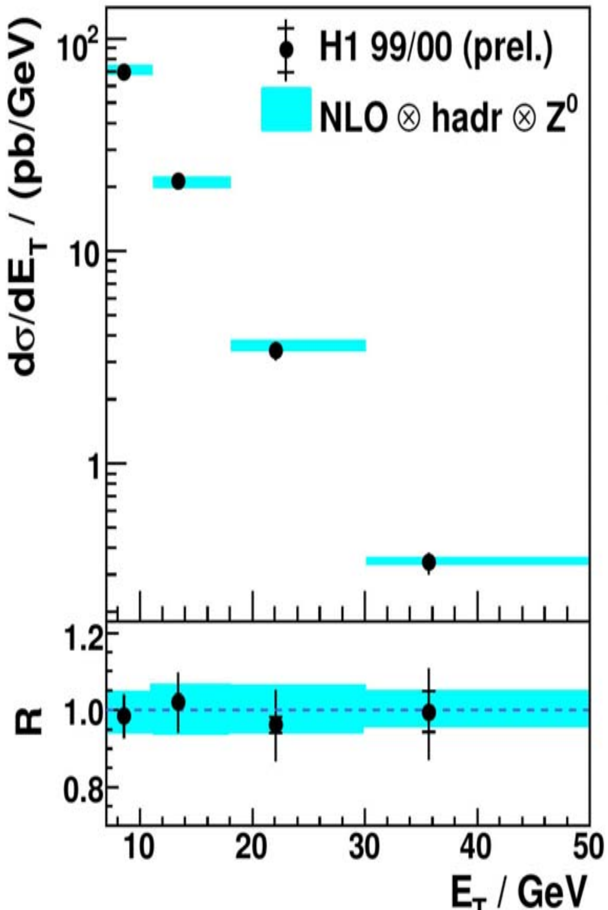


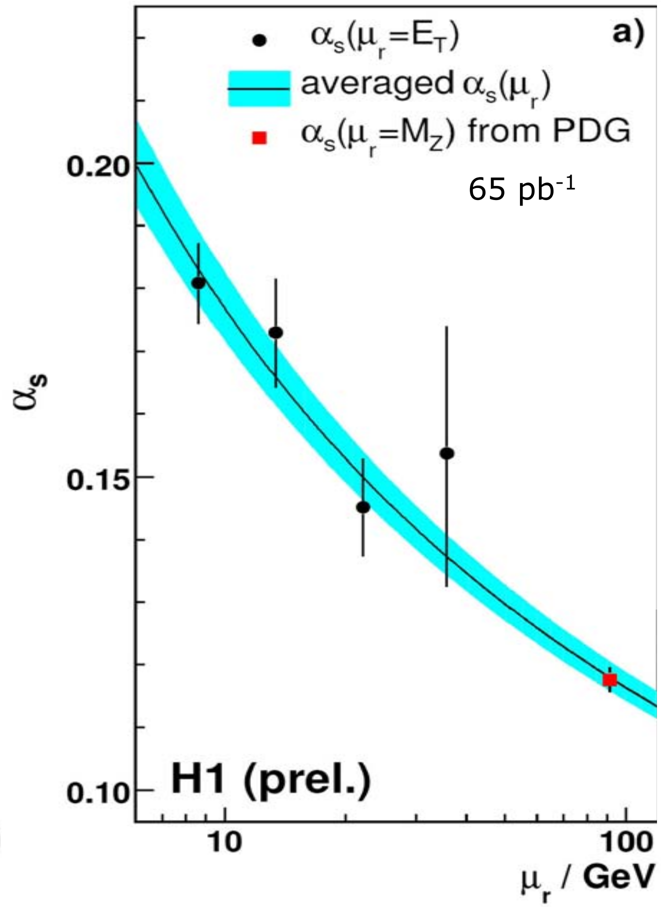


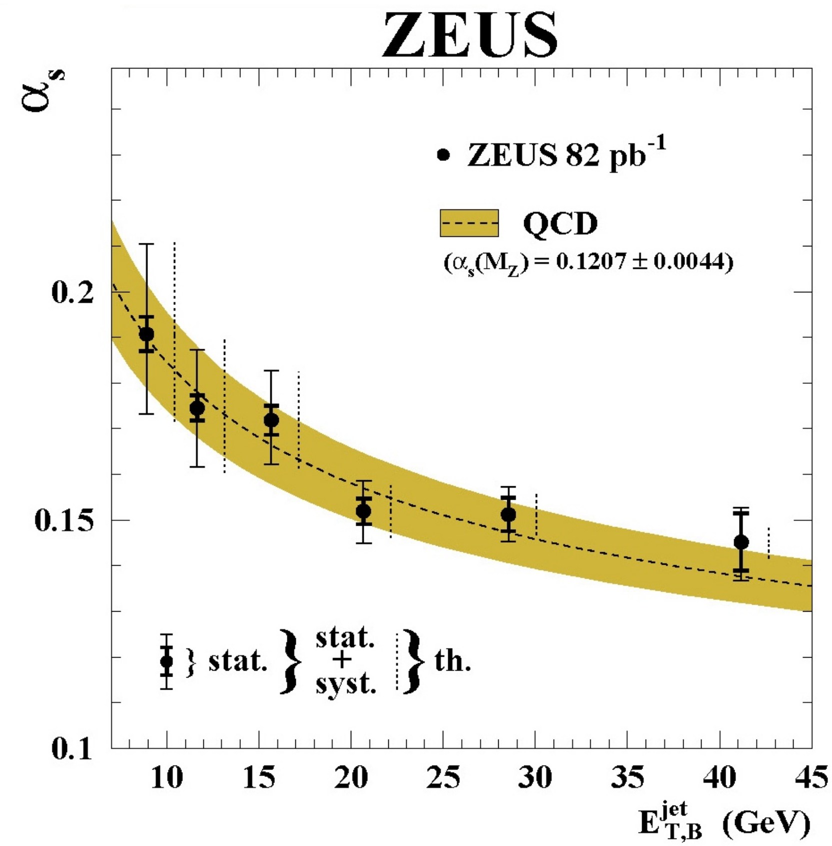


Good agreement with NLO

$\alpha_s(M_Z) = 0.1193 \ \pm 0.0014\,(\text{exp.})\ ^{+0.0046}_{-0.0032}\,(\text{th.})\ \pm 0.0016\,(\text{pdf.})$ **H1**

$\alpha_S(M_Z) = 0.1207 \pm 0.0014(\text{stat.}) \pm 0.0035(\text{syst.}) \pm 0.0023(\text{theo.})$ **ZEUS**

$\alpha_s(M_Z) = 0.1176 \pm 0.0020$ **PDG**

# Charm Production in DIS

Boson-gluon fusion process dominant

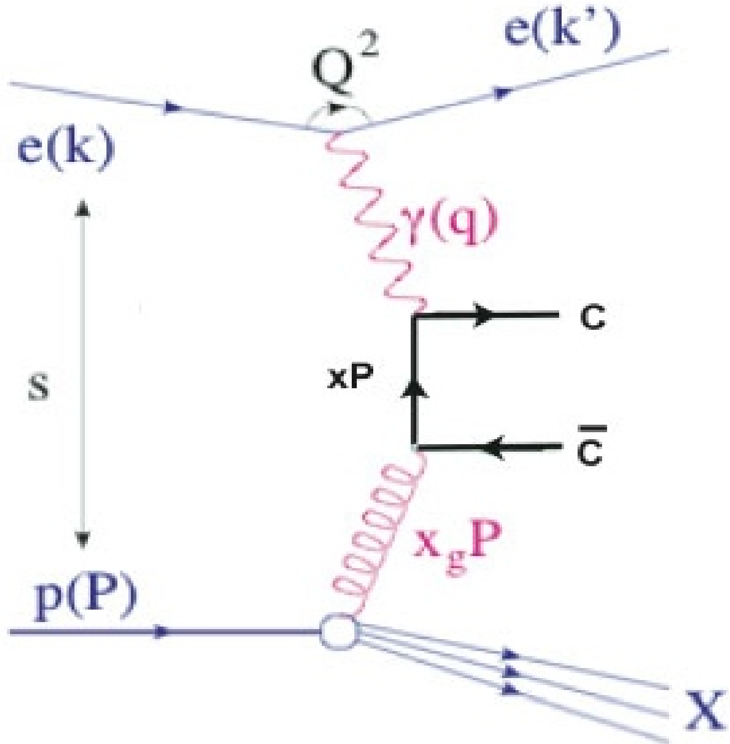


sensitive to gluon density

open charm contribution to $F_2$

New: $D^{*\pm}$ and $D^+$ from HERA II

e.g.: $D^*(2010) \to D^0\pi^+$ (68%) , $D^0 \to K^-\pi^+$ (4%)

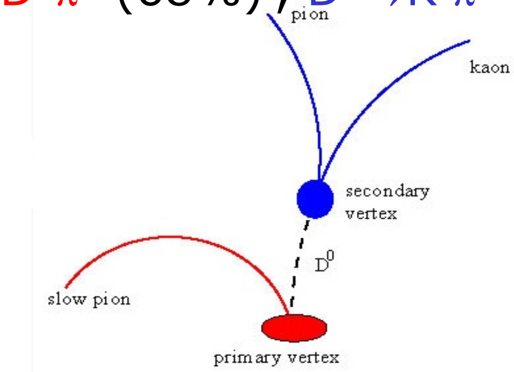


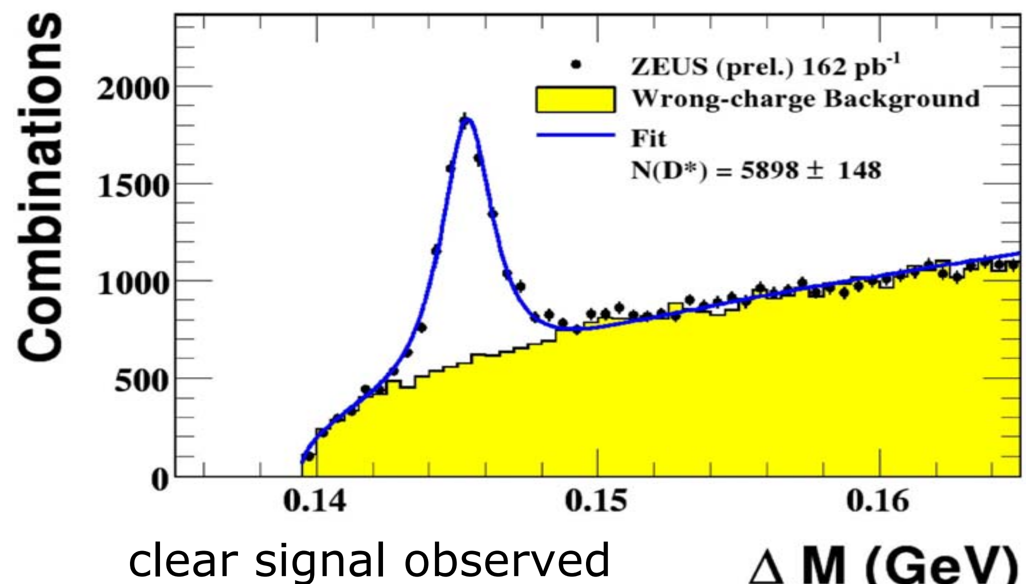


clear signal observed

# Charm Contribution to $F_2$

high precision measurements

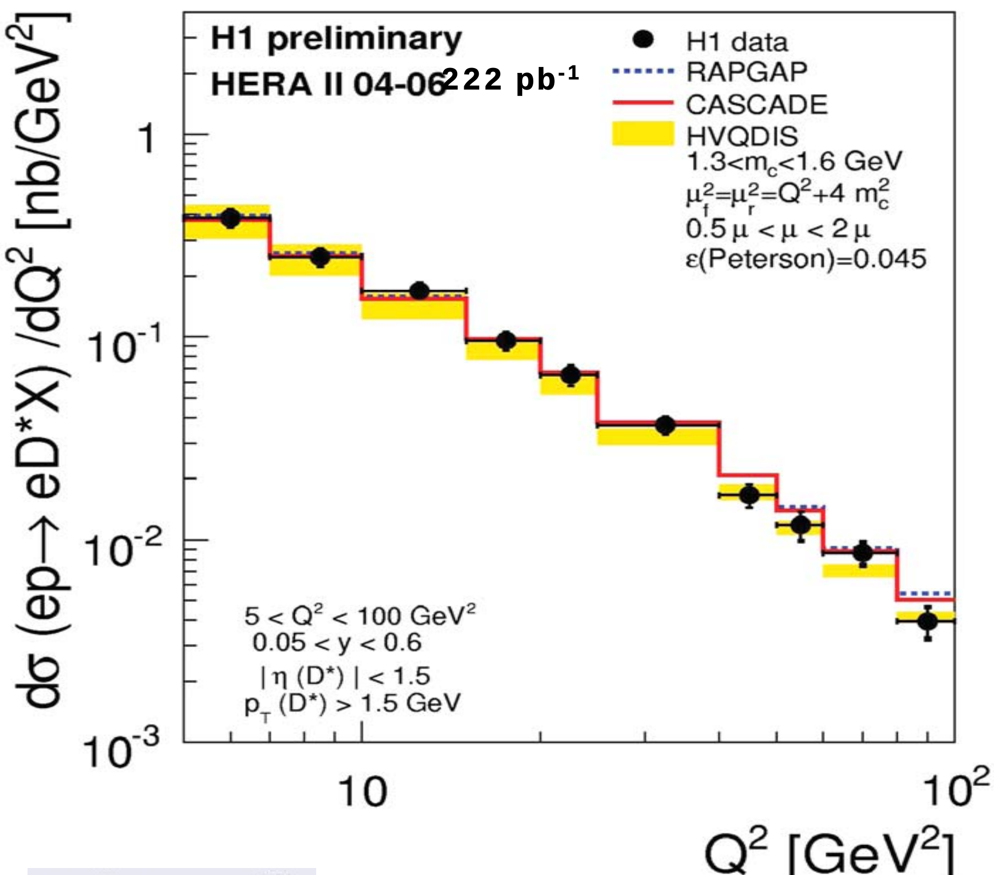


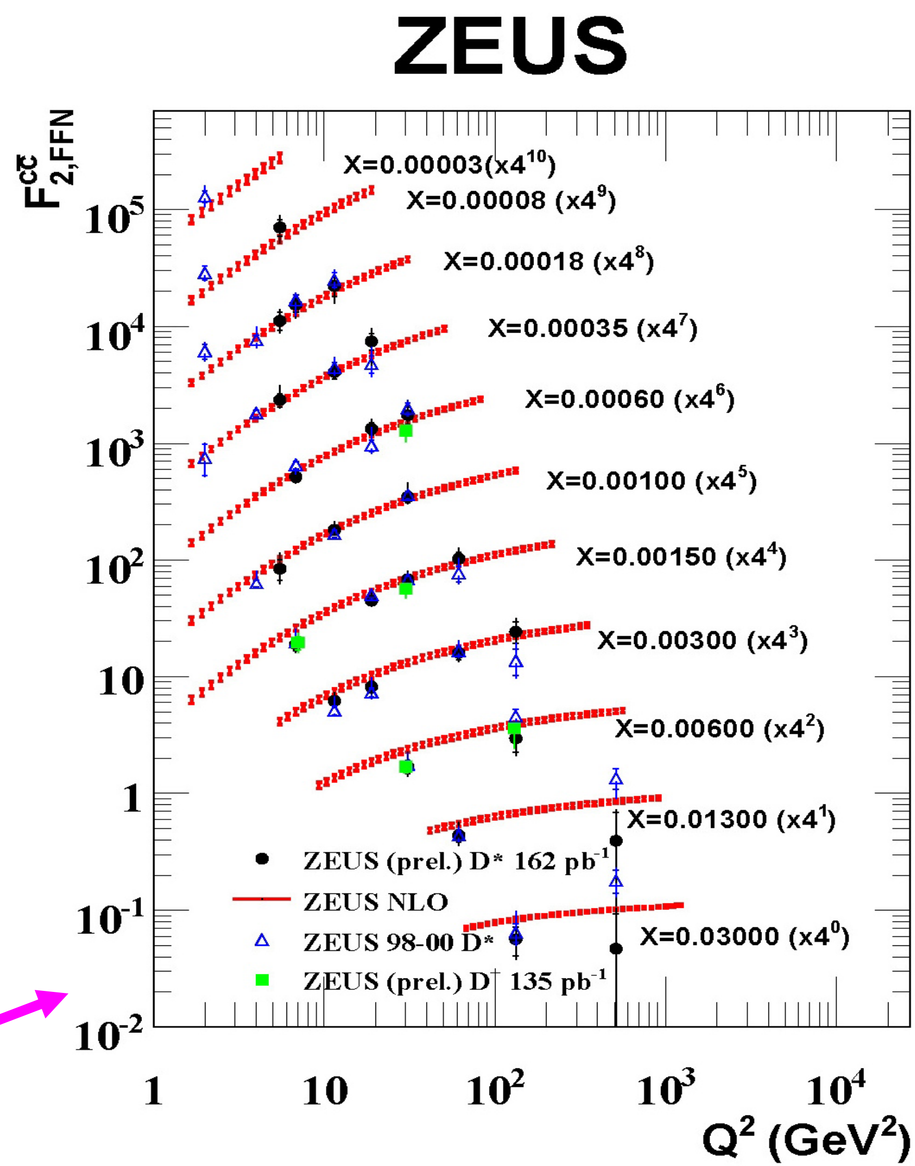


$F_2^{c\bar{c}}(x, Q^2)$ extrapolated to full $p_T$ and η phase space using HVQDIS (NLO QCD, B.W.Harris and J.Smith)

# Beauty Production in DIS

Preliminary, from μ+jet, D*μ, μμ measurements

from ZEUS HERA II data, 39 $pb^{-1}$

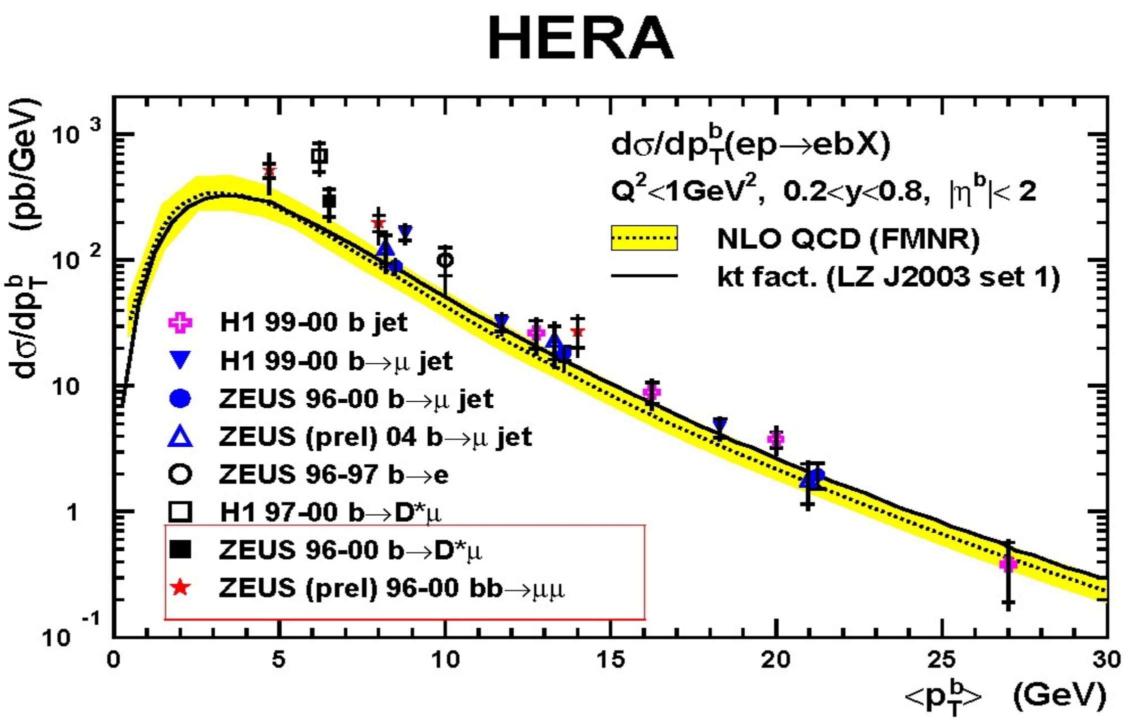


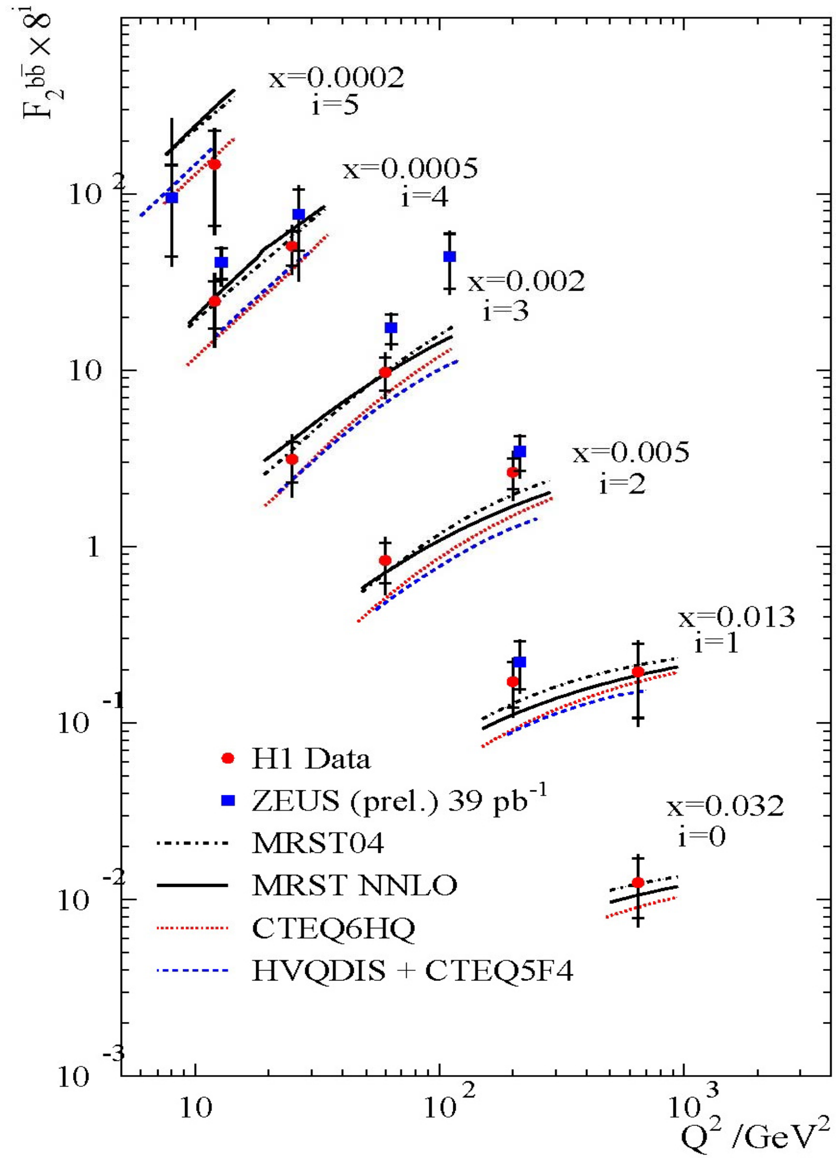

# 2001 ZEUS Upgrades

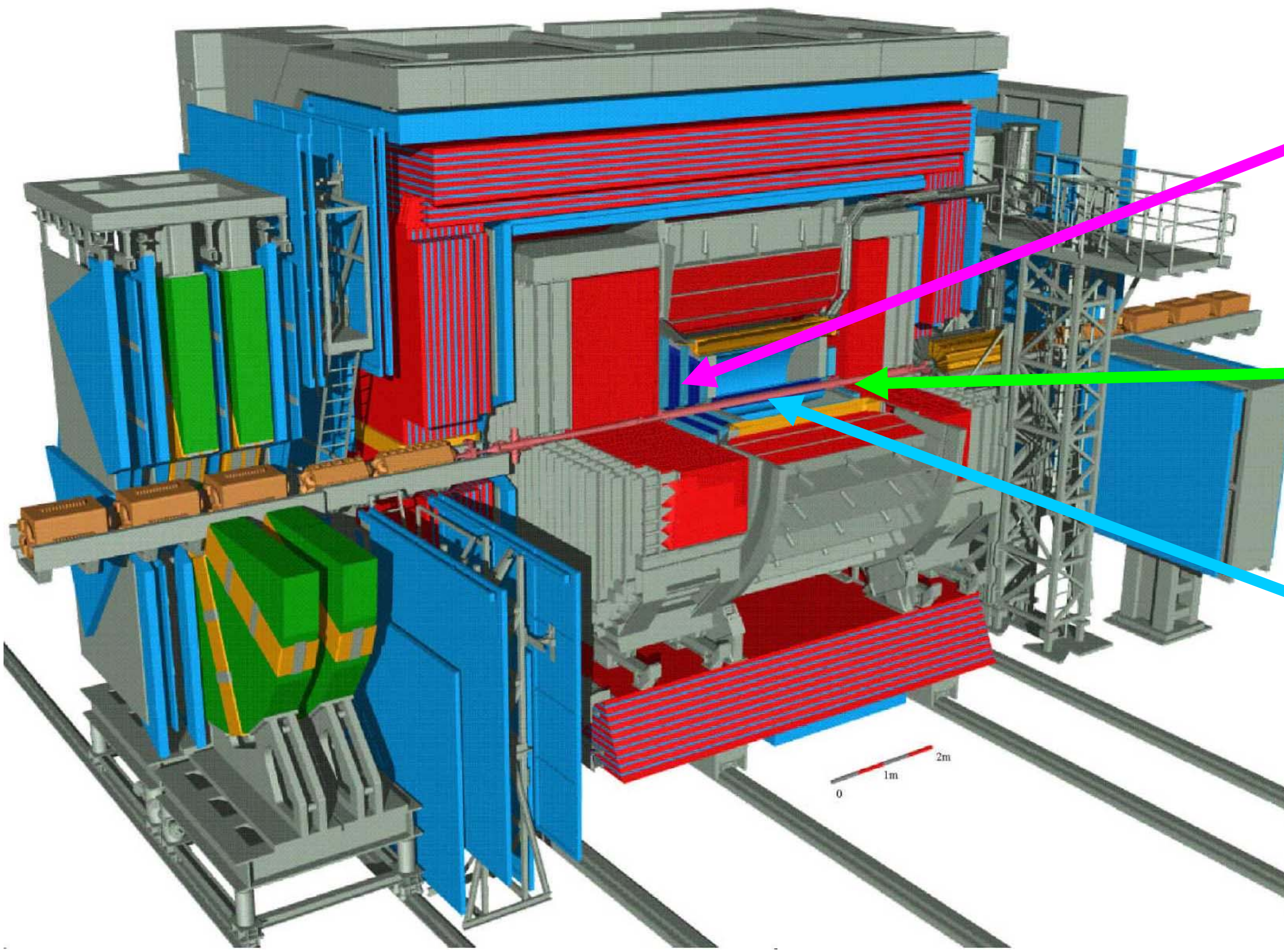


Straw Tube Forward Tracker (STT)

Beam pipe magnets

Micro Vertex Detector (MVD)

+Luminosity detector upgrades

# A Working Detector

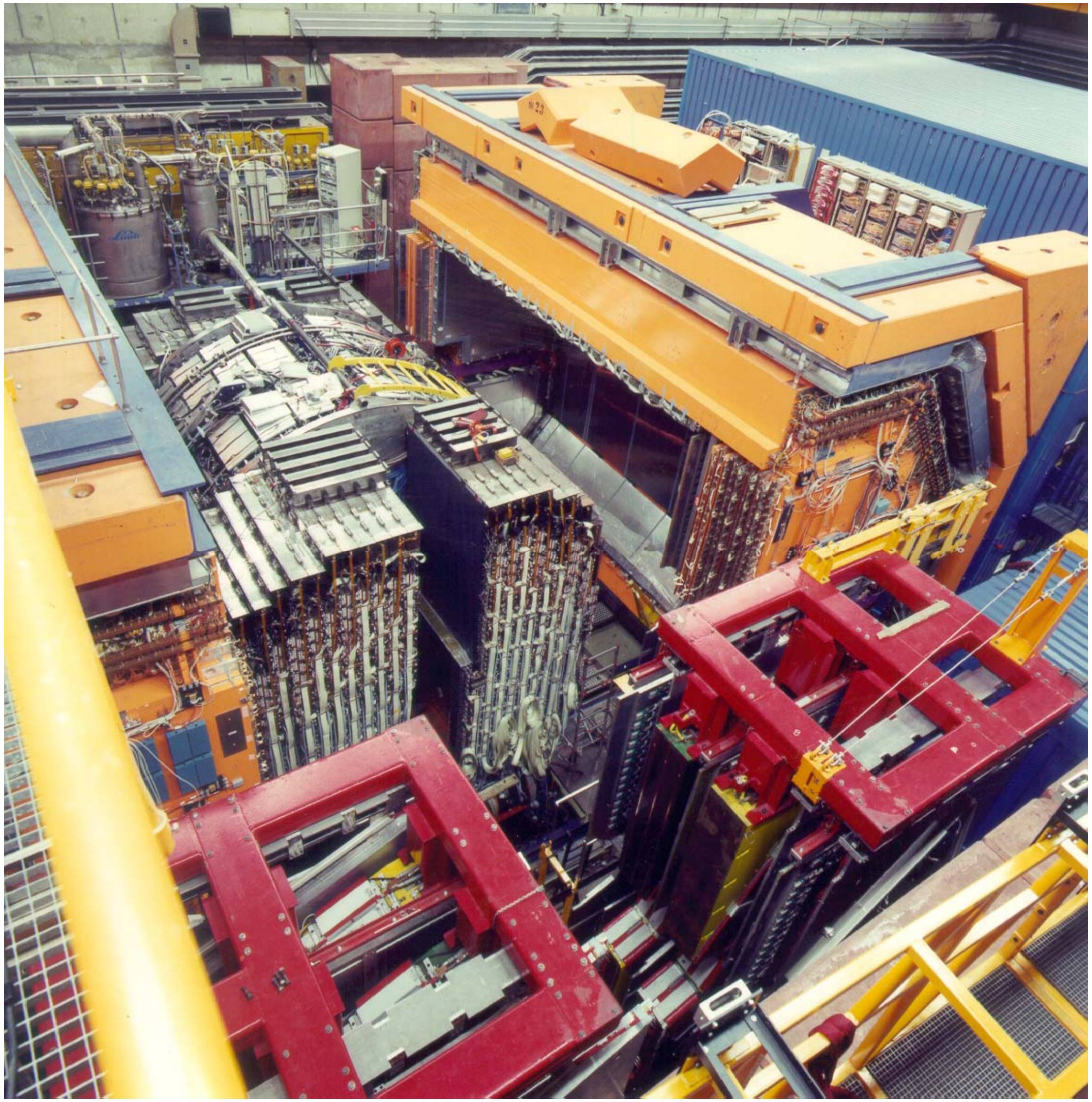

# Polarisation Measurement

The spin rotators convert the naturally building transverse polarisation (Sokolov-Turnov effects) to longitudinal polarisation at the locations of the detectors.

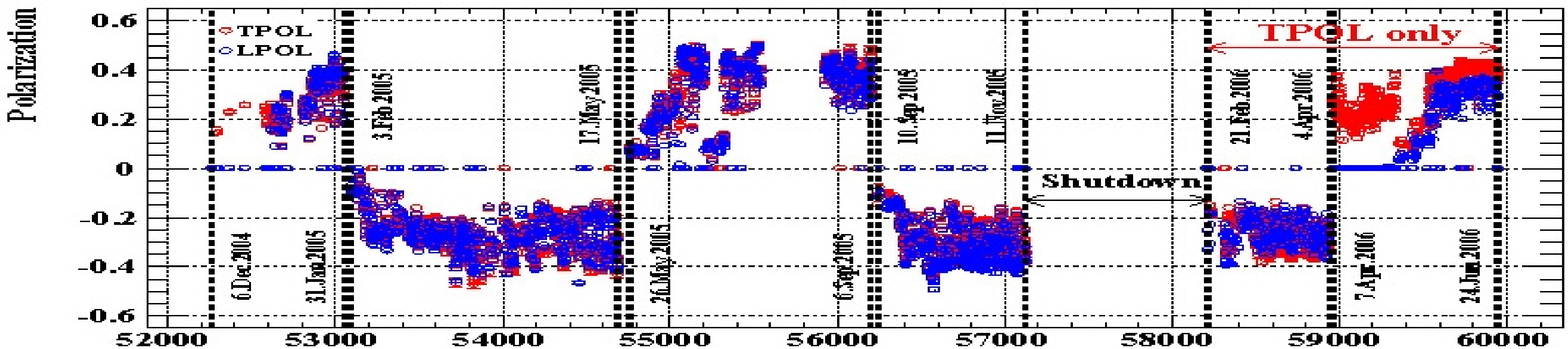


A laser light is Compton-scattered off the polarised e$^{\pm}$ beam

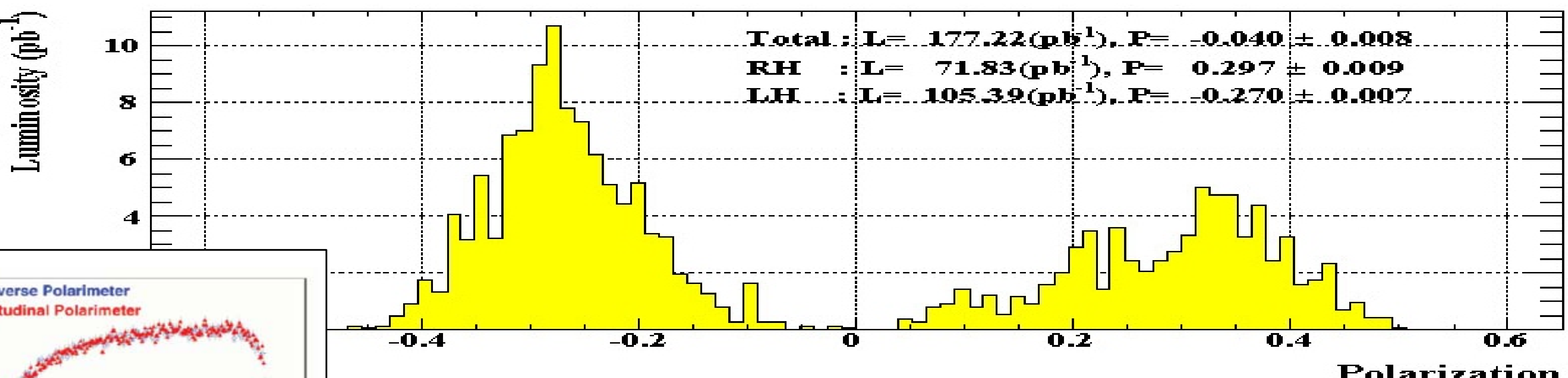


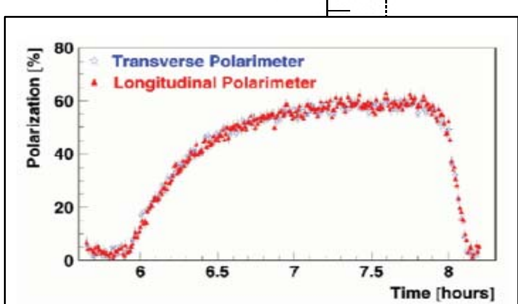


**TPOL** and **LPOL** are two independent polarimeters. Their operation is stable and reliable within ±1%.

# Data vs Monte-Carlo

Control plots: **black** points are the data
**blue** is the photoproduction background
yellow in the MC(ARIADNE) + photoproduction

good agreement

Q², y, $\theta_e$, $P_t^{had}$ / x, E', $\gamma_h$, Zvtx